J Physiol Sci
DOI 10.1007/s12576-011-0133-3

DNA microarray profiling identified a new role of growth hormone in vascular remodeling of rat ductus arteriosus

Mei-Hua Jin · Utako Yokoyama · Yoji Sato · Aki Shioda · Qibin Jiao · Yoshihiro Ishikawa · Susumu Minamisawa

Received: 3 December 2010 / Accepted: 28 December 2010

Abstract The ductus arteriosus (DA), a fetal arterial connection between the pulmonary artery and the aorta, has a character distinct from the adjacent arteries. We compared the transcriptional profiles of the DA and the aorta of Wistar rat fetuses on embryonic day 19 (preterm) and day 21 (near-term) using DNA microarray analyses. We found that 39 genes were expressed 2.5-fold greater in the DA than in the aorta. Growth hormone (GH) receptor (GHR) exhibited the most significant difference in expression. Then, we found that GH significantly promoted migration of DA smooth muscle cells (SMCs), thus enhancing the intimal cushion formation of the DA explants. GH also regulated the expression of cytoskeletal genes in DA SMCs, which may retain a synthetic phenotype in the smooth muscle-specific cytoskeletal genes. Thus, the present study revealed that GH-GHR signal played a role in the vascular remodeling of the DA.

Keywords Growth hormone · Gene expression · Vascular remodeling · Premature infant · Congenital heart disease

Introduction

The ductus arteriosus (DA), a fetal arterial connection between the pulmonary artery and the descending aorta, is essential to fetal life. The morphology and function of the DA dramatically change during development [1]. In particular, during late gestation, the deposition of extracellular matrix in the subendothelium is increased, and the smooth muscle cells (SMCs) of the media migrate into this region, resulting in intimal thickening [2]. This vascular remodeling of the DA is essential for its postnatal closure and is not observed in adjacent arteries. Thus, the DA has distinct characteristic features that differ from those of the adjacent arteries (the aorta and pulmonary arteries). This characteristic of the DA is largely dependent on the expression of the distinct subsets of genes involved in the developmental vascular remodeling that occurs during gestation. To understand the precise transcriptional network in the DA, genome-wide analysis is a powerful approach that can be utilized. In this context, several studies, including ours, have been carried out to identify the effects of oxygen [3] or maternal administration of vitamin A [4] on the transcriptional profiles of the DA. Although the study by Costa et al. [3] is the only one that demonstrated the characteristic differences in the transcriptional profiles between rat DA and the aorta of premature fetuses and neonates, they analyzed their transcriptional profiles on embryonic day 19 (e19) only; they did not examine the changes during later gestation.

Electronic supplementary material The online version of this article (doi:10.1007/s12576-011-0133-3) contains supplementary material, which is available to authorized users.

M.-H. Jin · U. Yokoyama · A. Shioda · Y. Ishikawa (✉) · S. Minamisawa (✉)
Cardiovascular Research Institute, Yokohama City University, 3-9 Fukuura, Kanazawa-ku, Yokohama 236-0004, Japan
e-mail: yishikaw@med.yokohama-cu.ac.jp

S. Minamisawa
e-mail: sminamis@waseda.jp

Y. Sato
Division of Cellular and Gene Therapy Products, National Institute of Health Sciences, 1-18-1 Kamiyoga, Setagaya-ku, Tokyo 158-8501, Japan

Q. Jiao · S. Minamisawa
Department of Life Science and Medical Bioscience, Waseda University Graduate School of Advanced Science and Engineering, 2-2 Wakamatsucho, Shinjuku-ku, Tokyo 162-8480, Japan

Published online: 02 February 2011

Because the morphological and physiological characteristics of the DA differ significantly between premature and mature fetuses [1], it is of great interest to investigate the transcriptional profiles of the DA and the adjacent aorta in the remodeling process that occurs during late gestation.

Materials and methods

Tissue collection for DNA microarray and quantitative reverse transcription polymerase chain reaction analyses

Pooled tissues from the DA or the aorta were obtained from Wistar rat embryos on e19 ($n \geq 120$) and e21 ($n \geq 120$). Reverse transcription polymerase chain reaction (RT-PCR) analysis was performed as described previously [2]. The information on PCR primers for RT-PCR analyses is provided in Supplemental data 1.

Total RNA preparation and DNA microarray analysis

Total RNA preparation and DNA microarray analysis were performed as described previously [4]. Briefly, total RNA was converted to biotin-labeled cRNA that was hybridized to rat genome U34A GeneChip DNA microarray (Affymetrix, Santa Clara, CA). The hybridization experiments were performed in duplicate and the intensities were averaged. If the difference in the signal intensities of a given sequence tag was equal to the cutoff (=2.5-fold) or more, and if the "Comparison Analysis" of the Microarray Suite Software indicated "increased" or "decreased" with the ≥2.5-fold difference at any developmental stage, that sequence tag was considered to exhibit a significant difference between the DA and the aorta.

Primary culture of rat DA SMCs

Vascular SMCs in primary culture were obtained from the DAs of Wistar rat embryos at e21. The tissues were minced and transferred to a 1.5-ml centrifuge tube that contained 800 μl of collagenase-dispase enzyme mixture [1.5 mg/ml collagenase-dispase (Roche), 0.5 mg/ml elastase type II-A (Sigma Immunochemicals, St. Louis, MO), 1 mg/ml trypsin inhibitor type I-S (Sigma), and 2 mg/ml bovine serum albumin fraction V (Sigma) in Hanks' balanced salt solution (Sigma)]. The digestion was carried out at 37°C for 15–20 min. Then cell suspensions were centrifuged, and the medium was changed to the collagenase II enzyme mixture [1 mg/ml collagenase II (Worthington), 0.3 mg/ml trypsin inhibitor type I–S, and 2 mg/ml bovine serum albumin fraction V in Hanks' balanced salt solution]. After 12 min of incubation at 37°C, cell suspensions were transferred to growth medium in 35-mm poly-L-lysine (Sigma)-coated dishes in a moist tissue culture incubator at 37°C in 5% CO_2, 95% ambient mixed air. The growth medium contained Dulbecco's modified Eagle's medium (DMEM) with 10% fetal bovine serum (FBS) and 1% penicillin-streptomycin solution (Sigma). The confluent cells were used at passages 4–6.

SMC migration assay

The migration assay was performed using 24-well Transwell culture inserts with polycarbonate membranes (8-μm pores; Corning Inc.) coated with fibronectin. The DA SMCs were harvested with trypsin-ethylenediamine tetraacetic acid (EDTA), resuspended in serum-free DMEM, and distributed at a density of 1×10^5 cells/100 μl in the inserts. The cells were allowed to settle in serum-free DMEM for 1 h before the addition of GH (20 and 200 ng/ml) in the lower chamber. Under basal conditions, the lower chambers were filled with 600 μl serum-free DMEM. SMCs were then allowed to migrate to the underside of the insert's membrane at 37°C/5% CO_2. At the end of the experiment, the cells were fixed in 10% buffered formalin. SMCs were stained with Cyto Quick (Muto Pure Chemicals), and cells on the upper surface of the membrane were mechanically removed with a cotton swab. Cells that migrated onto the lower surface of the membrane were manually counted from three different fields (0.5 mm^2/field) under a microscope.

Cell proliferation assays

[^{3}H]thymidine incorporation was used to measure cell proliferation in DA SMCs. The SMCs were reseeded into a 24-well culture plate at an initial density of 1×10^5 cells per well for 24 h before serum starvation with DMEM containing 0.1% FBS. Cells were then incubated with or without GH (20 and 200 ng/ml) for 24 h in the starvation medium before addition of 1 μCi of [*methyl*-^{3}H]thymidine (specific activity 5 Ci/mM; Amersham International, Bucks, UK) for 4 h at 37°C. After fixation with 1.0 ml of 10% trichloroacetic acid, the cells were solubilized with 0.5 ml of 0.5 M NaOH and then neutralized with 0.25 ml of 1 N HCl. A liquid scintillation counter was used to measure [^{3}H]thymidine incorporation. Data obtained from triplicate wells were averaged.

Quantitation of hyaluronan

The amount of hyaluronan in the cell culture supernatant was measured by a latex agglutination method based on the specific interaction of hyaluronan with the latex-labeled hyaluronan-binding protein from bovine cartilage (Fujirebio Inc.). Hyaluronan was quantified in duplicate according to

the manufacturer's instructions using 2.5-μl aliquots of the conditioned cell culture medium using the HITACHI 7070 analysis system (Hitachi) at an 800-nm wavelength.

Organ culture

Fetal arteries including the DA and the aortic arch arteries were incubated with GH (200 ng/ml) for 72 h in serum-free DMEM as described previously [2]. Explants were then fixed in 10% buffered formalin and embedded in paraffin. The sectioned segments in the middle portion of the DA were analyzed histochemically.

Immunohistochemistry

Tissue staining and immunohistochemistry were performed as described previously [5, 6]. Mouse monoclonal anti-GHR antibody (MAB263) was purchased from Abcam (Tokyo, Japan).

Statistics

Data are presented as mean ± standard error (SEM) of independent experiments. Statistical analysis was performed between two groups by unpaired two-tailed Student's *t* test or unpaired *t* test with Welch correction, and among multiple groups by one-way analysis of variance (ANOVA) followed by Neuman-Keuls multiple comparison test. A p value of <0.05 was considered significant.

Results

Genes differentially expressed between the DA and the aorta

All the microarray data in the present study were deposited at the Gene Expression Omnibus (GEO) repository (http://www.ncbi.nlm.nih.gov/projects/geo/; accession no. GSE3422). A total of 117 genes (142 probe sets) showed a significant difference (≥2.5-fold) between the DA and the aorta at e19 or e21. Among 117 genes, 39 (43 probe sets) exhibited a DA-dominant expression pattern (Table 1), and 78 (99 probe sets) exhibited an aorta-dominant expression pattern (Table 2).

Of 39 genes in the DA-dominant expression pattern (Table 1), 34 had a known function, and 3 were homologous to known genes. Although several genes, such as prostaglandin E receptor 4 (subtype EP4) (Ptger4) and endothelin-1, are known to play an important role in the regulation of vascular tone of the DA [1], the role of most of the other genes in the DA has not been identified. We found that growth hormone (GH) receptor exhibited the highest difference in the expression between the DA and the aorta among 39 DA-dominant genes.

Of the 39 genes, 9 encode proteins related to cytoskeleton and the extracellular matrix, including sarcomeric genes such as Myh11 (myosin heavy chain 11), Myl6 (myosin light chain, polypeptide 6, alkali, smooth muscle and non-muscle), Actg2 (actin, gamma 2), Tpm1 (tropomyosin 1, alpha), Tnn (tenascin N, predicted), and Lamb2 (laminin beta2). Three membrane ion channels, ATPase Na^+/K^+ transporting b1 polypeptide and potassium inwardly rectifying channel (Atp1b1), subfamily J, member 8 (Kcnj8), which is known as ATP-sensitive potassium channel K_{ATP}-1, and Ca^{2+} channel, voltage-dependent, $\alpha 2/\delta$ subunit 1 (Cacna2d1), were also strongly expressed in the DA.

We also identified 79 genes in the aorta-dominant expression pattern (Table 2). Of the 79 genes, 14 genes encode proteins related to cytoskeleton and the extracellular matrix. Cardiac sarcomeric genes such as Myh6 (myosin heavy chain, polypeptide 6), Myh7 (myosin heavy chain, polypeptide 7), Myl7 (myosin, light polypeptide 7, regulatory), Myl2 (myosin regulatory light chain 2, ventricular/cardiac muscle isoform), Actc1 (alpha, actin alpha cardiac 1), Tnnt2 (troponin T2, cardiac), Tnni3 (troponin I, cardiac), and Fn1 (fibronectin 1) were more highly expressed in the aorta than in the DA. Accordingly, there was a marked difference in the composition of the genes related to the cytoskeleton and the extracellular matrix between the DA and the aorta. Sixteen genes were expressed 2.5-fold more in the aorta at both e19 and e21 than in the DA, whereas 24 genes were expressed 2.5-fold more in the aorta than in the DA only at e21. To confirm the results of the DNA microarray, we performed RT-PCR (Supplemental data 2).

Growth hormone receptor mRNA and protein were dominantly expressed in the developing DA

As mentioned above, GH receptor (GHR) exhibited the highest difference of expression between the DA and the aorta (Fig. 1a), suggesting that GH-GHR signal plays a distinct role in the vascular remodeling of the DA from the aorta. The expression of GH mRNA was very low, and there was no difference between the DA and the aorta (Fig. 1b). Interestingly, the expression levels of insulin-like growth factor (IGF)-I and IGF-II mRNAs were higher in the aorta than in the DA, whereas the expression levels of IGF-I receptor (IGF-IR) and IGF-IIR mRNAs did not differ (Fig. 1c–f). In addition, the expression levels of IGF binding protein (IGFBP) 2 and IGFBP5 mRNAs were also higher in the aorta than in the DA at e21 and at e19, respectively (Table 2).

The expression of GHR mRNA was also confirmed by quantitative RT-PCR analyses. We found that the expression levels of GHR mRNA were higher in the rat DA than

Table 1 DA-dominant genes

	Probe set ID	RefSeq Transcript ID	Gene title	Gene symbol	Fold difference between DA and aorta	
					e19	e21
1	**rc_AI104225_at**	**NM_017094**	**Growth hormone receptor**	**Ghr**	**5.0**	**8.7**
2	Z83757mRNA_at	XM_222794	Tenascin N (predicted)	Tnn_predicted	2.3	7.4
3	L16764_s_at/// Z75029_s_at	NM_031971/// NM_212504	Heat shock 70kD protein 1A///heat shock 70kD protein 1B	Hspa1a///Hspa1b	8.6	7.1
4	rc_AA891527_at	NM_022531	Desmin	Des	1.4	6.3
5	rc_AA893846_at	NM_053591	Dipeptidase 1 (renal)	Dpep1	3.4	5.6
6	X73524_at	NM_013129	Interleukin 15	Il15	2.0	5.6
7	D28561_s_at	NM_031677	Four and a half LIM domains 2	Fhl2	3.4	4.9
8	rc_AA894200_at	XM_342032	Proprotein convertase subtilisin/kexin type 5	Pcsk5	1.4	4.8
9	AF002281_at	NM_012870	Tumor necrosis factor receptor superfamily, member 11b (osteoprotegerin)	Tnfrsf11b	1.2	4.7
10	M22323_at	NM_013086/// NM_017334	cAMP responsive element modulator	Crem	1.8	3.5
11	U94330_at	NM_001007678	Mss4 protein	Mss4	1.5	3.1
12	rc_AA799773_at	NM_134410	Mg87 protein	Mg87	1.3	2.9
13	X82152_at	NM_001002287	MAS-related G protein-coupled receptor, member B4	Mrgprb4	2.5	2.9
14	M64711_at	NM_080698	Fibromodulin	Fmod	1.6	2.8
15	D28860_s_at	NM_012893	Actin, gamma 2	Actg2	3.7	2.8
16	U69272_g_at	NM_017099	Potassium inwardly rectifying channel, subfamily J, member 8	Kcnj8	2.8	2.8
17	rc_AA859578_at	NM_021587	Latent transforming growth factor beta binding protein 1	Ltbp1	2.0	2.7
18	rc_AA859954_at	NM_012751	Solute carrier family 2 (facilitated glucose transporter), member 4	Slc2a4	2.3	2.7
19	rc_AI014135_g_at	NM_013113	ATPase, Na +/K + transporting, beta 1 polypeptide	Atp1b1	2.1	2.7
20	rc_AI176662_s_at	NM_019131	Tropomyosin 1, alpha	Tpm1	2.3	2.7
21	AB020504_g_at	NM_032076	Prostaglandin E receptor 4 (subtype EP4)	Ptger4	2.4	2.6
22	rc_AI232078_at	NM_012827	Bone morphogenetic protein 4	Bmp4	2.8	2.6
23	U02553cds_s_at	NM_033485	PRKC, apoptosis, WT1, regulator	Pawr	1.4	2.6
24	X63253cds_s_at	NM_080902	Hypoxia induced gene 1	Hig1	1.7	2.6
25	M60921_g_at	XR_086177	PMF32 protein (predicted)	Pmf31	2.8	2.5
26	S66024_at	XM_343144	Myosin, light polypeptide 6, alkali, smooth muscle and non-muscle (predicted)	Myl6_predicted	2.7	2.5
27	M86621_at	NM_012887	Thymopoietin	Tmpo	1.2	2.5
28	X54686cds_at/// rc_AA891041_at	XM_573030	Myosin heavy chain 11	Myh11	3.7	2.3
29	U17254_g_at	NM_012974	Laminin, beta 2	Lamb2	2.5	2.3
30	Z22607_at	NM_019620	Zinc finger protein 386 (Kruppel-like)	Znf386	7.5	2.2
31	rc_AA891422_at	NM_053650	PDZ and LIM domain 3	Pdlim3	2.6	1.8
32	rc_AI144767_s_at/// rc_AA875132_at	NM_024162	Fatty acid binding protein 3	Fabp3	3.5	1.7
33	M63656_s_at	NM_012919	Calcium channel, voltage-dependent, alpha2/delta subunit 1	Cacna2d1	2.7	1.6
34	rc_AI014163_at	NM_012548	Endothelin 1	Edn1	2.8	1.4
35	rc_AI639161_at	XM_346029	Similar to KIAA1411 protein (predicted)	RGD1304927_predicted	2.7	1.2
36	rc_AA866345_at	NM_012531	Catechol-*O*-methyltransferase	Comt	4.6	1.2
37	rc_AI230614_s_at/// rc_AI112173_at	NM_001002829	RAS-like family 11 member A	Rasl11a	3.0	1.1
38	rc_AA799511_g_at	–	–	–	1.8	2.6
39	rc_AA893871_at	–	–	–	1.4	2.5

Table 2 Aorta-dominant genes

	Probe set ID	RefSeq transcript ID	Gene title	Gene symbol	Fold difference between aorta and DA	
					e19	e21
1	X15939_r_at///rc_AI104924_f_at/// rc_AI103920_f_at///rc_AA891522_f_at	NM_017239	Myosin heavy chain, polypeptide 6, cardiac muscle, alpha	Myh6	2.2	23.8
2	X80130cds_i_at///rc_AI104567_g_at/// rc_AA866452_s_at	XM_215801	Actin alpha cardiac 1	Actc1	3.0	18.4
3	M93638_at	NM_183333	Keratin complex 2, basic, gene 5	Krt2-5	6.9	16.8
4	rc_AA891242_g_at///rc_AA891242_at	NM_001106017	Myosin, light polypeptide 7, regulatory	Myl7	3.2	15.3
5	X15939_f_at	NM_017240	Myosin, heavy polypeptide 7, cardiac muscle, beta	Myh7	1.9	13.2
6	D78159mRNA_s_at	NM_001008806	Type II keratin Kb4	Kb4	1.5	9.1
7	X15512_at	NM_012824	Apolipoprotein C–I	Apoc1	0.5	7.4
8	U67914_at	XM_342219	Carboxypeptidase A3	Cpa3	1.7	7.2
9	rc_AI169372_g_at	NM_031839	Cytochrome P450, family 2, subfamily c, polypeptide 23	Cyp2c23	0.5	5.5
10	K01933_at	NM_012582	Haptoglobin	Hp	0.5	5.1
11	M80829_at	NM_012676	Troponin T2, cardiac	Tnnt2	1.3	4.8
12	X00975_g_at///X07314cds_at	NM_001035252	Myosin, light polypeptide 2	Myl2	5.1	4.8
13	M24852_at	NM_013002	Purkinje cell protein 4	Pcp4	4.7	4.8
14	M92074_g_at	NM_017144	Troponin I, cardiac	Tnni3	2.1	4.6
15	rc_AA945054_s_at	NM_022245	Cytochrome b-5	Cyb5	0.8	4.1
16	S76779_s_at	NM_138828	Apolipoprotein E	Apoe	1.3	3.9
17	AF014503_at	NM_053611	Nuclear protein 1	Nupr1	3.2	3.9
18	X02412_at	NM_019131	Tropomyosin 1, alpha	Tpm1	1.0	3.7
19	D00752_at	NM_182474	Serine protease inhibitor	Spin2a	0.5	3.6
20	D89730_at	NM_001012039	Epidermal growth factor-containing fibulin-like extracellular matrix protein 1 (predicted)	Efemp1_predicted	4.0	3.6
21	M14656_at	NM_012881	Secreted phosphoprotein 1	Spp1	4.7	3.4
22	X81448cds_at///rc_AI072634_at	NM_053976	Keratin complex 1, acidic, gene 18	Krt1-18	1.5	3.1
23	rc_AA946368_at	XM_575338	Similar to fatty acid translocase/CD36	LOC499984	1.9	3.1
24	M91595exon_s_at///J04486_at/// A09811cds_s_at	NM_013122	Insulin-like growth factor binding protein 2	Igfbp2	2.1	3.1
25	U30938_at	NM_013066	Microtubule-associated protein 2	Mtap2	2.1	3.0
26	Y12502cds_at	NM_021698	Coagulation factor XIII, A1 subunit	F13a	2.8	2.9
27	M84719_at	NM_012792	Flavin containing monooxygenase 1	Fmo1	4.4	2.8
28	M91652complete_seq_at	NM_017073	Glutamine synthetase 1	Glul	1.8	2.8
29	J03752_at	NM_134349	Microsomal glutathione *S*-transferase 1	Mgst1	1.1	2.7
30	AF072411_g_at///rc_AA925752_at	NM_031561/// XM_575338/// XM_575339	CD36 antigen///similar to fatty acid translocase/CD36///similar to fatty acid translocase/CD36	Cd36///LOC499984/// LOC499985	1.7	2.7
31	L19998_g_at//L19998_at	NM_031834	Sulfotransferase family 1A, phenol-preferring, member 1	Sult1a1	2.9	2.7
32	L25387_g_at	NM_206847	Phosphofructokinase, platelet	Pfkp	1.7	2.6
33	rc_AI230247_s_at	NM_019192	Selenoprotein P, plasma, 1	Sepp1	2.2	2.6
34	rc_AI237731_s_at///L03294_g_at///L03294_at	NM_012598	Lipoprotein lipase	Lpl	0.9	2.6
35	M83680_at	NM_053589	RAB14, member RAS oncogene family	Rab14	2.6	2.6
36	rc_AI639532_at	XM_215935	Troponin C2, fast (predicted)	Tnnc2_predicted	4.7	2.5
37	X71127_g_at	NM_019262	Complement component 1, q subcomponent, beta polypeptide	C1qb	3.2	2.5
38	AB000113_at	NM_017217	Solute carrier family 7 (cationic amino acid transporter, y + system), member 3	Slc7a3	1.6	2.5
39	rc_AA894092_at	XM_342245	Periostin, osteoblast specific factor (predicted)	Postn_predicted	2.5	2.5
40	M32062_g_at	NM_053843/// XM_573502/// XM_573503	Fc receptor, IgG, low affinity III///Fc gamma receptor II beta///similar to low affinity immunoglobulin gamma Fc region receptor III precursor (IgG Fc receptor III) (Fc-gamma RIII) (FcRIII)	Fcgr3/// LOC498276/// LOC498277	3.2	2.4
41	M24353_g_at	XM_343636	Mannosidase 2, alpha 1	Man2a1	4.7	2.3

Table 2 continued

	Probe set ID	RefSeq transcript ID	Gene title	Gene symbol	Fold difference between aorta and DA	
					e19	e21
42	U77931_at	NM_147136	rRNA promoter binding protein	RGD:727924	3.0	2.3
43	M12098_s_at	NM_012604	Myosin, heavy polypeptide 3, skeletal muscle, embryonic	Myh3	2.7	2.1
44	AJ005396_at	XM_342325	Procollagen, type XI, alpha 1	Col11a1	3.1	2.1
45	rc_AA893230_at	XM_236325	Ceroid-lipofuscinosis, neuronal 6 (predicted)	Cln6_predicted	2.8	2.1
46	rc_AA875172_at	NM_053360	SH3-domain kinase binding protein 1	Sh3kbp1	2.6	2.1
47	AB012235_at///AB012234_g_at/// AB012234_at	XM_213849	Nuclear factor I/X	Nfix	4.9	1.9
48	X00722_at	XM_578812	Similar to testin	LOC503278	2.8	1.9
49	M32062_at	NM_053843/// XM_573502	Fc receptor, IgG, low affinity III///Fc gamma receptor II beta	Fcgr3///LOC498276	2.8	1.8
50	rc_AI013472_at///rc_AA924925_at	NM_138905	ER transmembrane protein Dri 42	Ppap2b	2.6	1.8
51	U62897_at	NM_012836	Carboxypeptidase D	Cpd	3.0	1.8
52	Z12298cds_s_at///X59859_r_at///X59859_i_at	NM_024129	Decorin	Dcn	2.7	1.7
53	M15797_at	XM_213954	Nidogen (entactin)	Nid	13.4	1.7
54	AF041066_at	NM_020082	Ribonuclease, RNase A family 4	Rnase4	2.9	1.7
55	U50842_at	XM_343427	Neural precursor cell expressed, developmentally downregulated gene 4A	Nedd4a	3.9	1.6
56	rc_AA866443_at	NM_001008560	Protease, serine, 35 (predicted)	Prss35	4.2	1.6
57	S66184_s_at///rc_AI234060_s_at/// rc_AI102814_at///rc_AA875582_at	NM_017061	Lysyl oxidase	Lox	3.2	1.6
58	rc_AI639314_at	XM_238213	Delangin (predicted)	NIPBL_predicted	2.5	1.6
59	rc_AA800908_at	XM_344450	Potassium channel tetramerisation domain containing 12 (predicted)	Kctd12_predicted	3.6	1.6
60	rc_AI029920_s_at	NM_012817	Insulin-like growth factor binding protein 5	Igfbp5	4.0	1.5
61	L10326_at	NM_019132	GNAS complex locus	Gnas	2.7	1.5
62	E00988mRNA_s_at	NM_031511	Insulin-like growth factor 2	Igf2	3.0	1.4
63	U01908cds_s_at///D43778exon#3_s_at/// D16840_s_at	NM_012494	Angiotensin II receptor, type 2	Agtr2	4.4	1.4
64	rc_AI176461_s_at	NM_017211	Golgi apparatus protein 1	Glg1	3.3	1.4
65	U23146cds_s_at	NM_057103	A kinase (PRKA) anchor protein (gravin) 12	Akap12	2.9	1.4
66	rc_AA900750_s_at	NM_012760	Pleiomorphic adenoma gene-like 1	Plagl1	2.5	1.4
67	Z17223_at	NM_017149	Mesenchyme homeo box 2	Meox2	2.6	1.3
68	rc_AI171966_at	NM_198740	Major histocompatibility complex, class II, DM beta	RGD:735096	2.5	1.2
69	U35775_g_at///U35775_at	NM_031552	Adducin 3 (gamma)	Add3	5.3	1.2
70	U43534_at	NM_012894	Adenosine deaminase, RNA-specific, B1	Adarb1	2.7	0.8
71	AF004811_at	NM_030863	Moesin	Msn	2.9	0.7
72	X05831cds_at///U82612cds_at///M28259cds_at	NM_019143	Fibronectin 1	Fn1	3.9	0.7
73	U17604_at	NM_053865	Reticulon 1	Rtn1	2.6	0.7
74	X51531cds_g_at///X51531cds_at	–	–	–	4.4	30.2
75	rc_AA799865_at	–	Transcribed locus	–	1.3	2.7
76	X05472cds#2_at	–	–	–	7.2	2.4
77	rc_AA799406_at	XM_578859	Hypothetical protein LOC503325	LOC503325	2.6	1.3
78	rc_AA859921_at	–	–	–	3.3	0.9

in the aorta at e19 and at e21 ($p < 0.05$ and $p < 0.001$, $n = 6$–8, respectively) (Fig. 2a).

We then examined the localization of GHR in the DA and the aorta at e19 and e21. GHR immunoreactivity was detected abundantly in the SMC layer and less in the endothelial cells of the DA (Fig. 2b).

GH promoted DA SMC migration, but not proliferation

SMC migration and proliferation play an essential role in intimal cushion formation of the DA, especially during late gestation. Therefore, we investigated the effects of GH on migration and proliferation using DA SMCs in primary

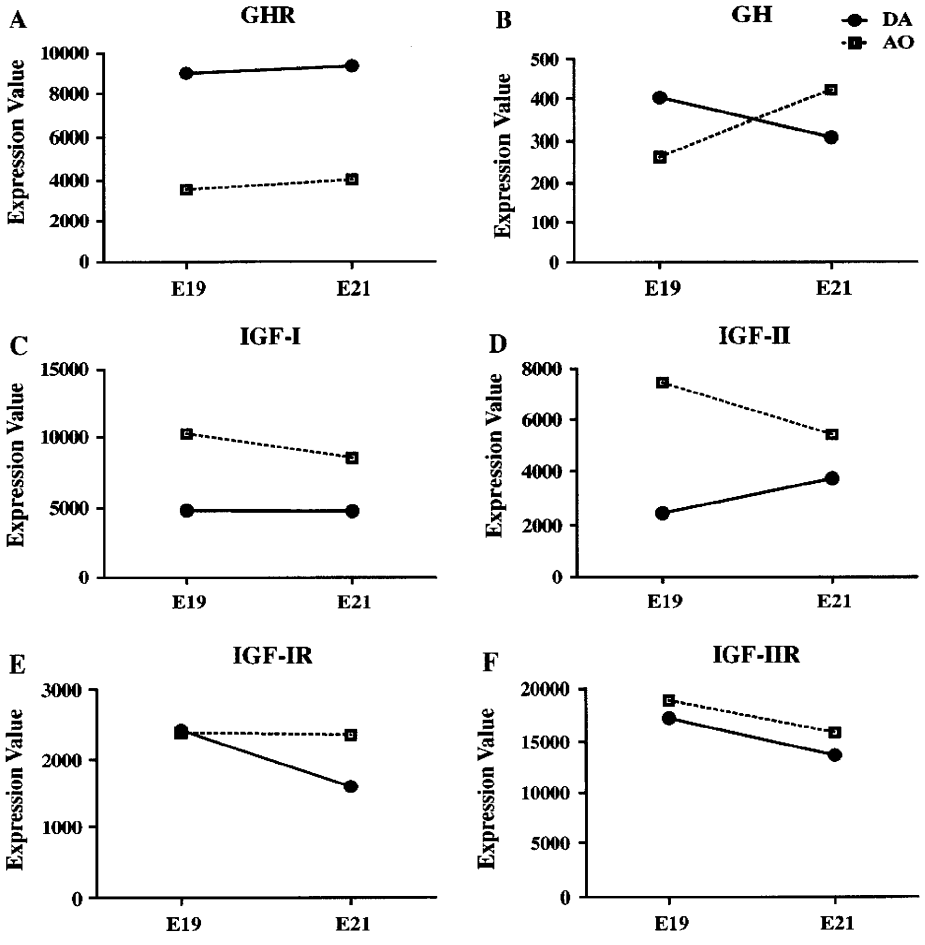

Fig. 1 The expression of growth hormone receptor and its related genes in the developing DA by DNA microarray analysis. **a** GHR (growth hormone receptor), **b** GH (growth hormone), **c** IGF (insulin-like growth factor)-I, **d** IGF-II, **e** IGF-IR (type I receptor), and **f** IGF-IIR (type II receptor) mRNA. *E19* Embryonic day 19, *E21* embryonic day 21, *DA* ductus arteriosus, *AO* aorta

culture from rat DA at e21. We found that recombinant rat GH promoted migration of DA SMCs in a dose-dependent manner (Fig. 3a). However, the same amount of GH did not promote migration of aortic SMCs (Supplemental data 3). When DA SMCs were treated with platelet-derived growth factor BB (PDGF-BB) (10 ng/ml), a potent stimulator for SMC migration, SMC migration was significantly increased by 141% in DA SMCs. In contrast, [^{3}H]thymidine incorporation was unchanged in DA SMCs in the presence of recombinant rat GH (up to 200 ng/ml) (Fig. 3b). When DA SMCs were treated with 10% FBS, a potent stimulator for SMC proliferation, [^{3}H]thymidine incorporation was significantly increased by 112% in DA SMCs. Hyaluronan is an important component of the intimal cushion, and hyaluronan-rich matrices are essential for cell migration and proliferation in the DA [2]. Because our recent study revealed that PGE_1 is a potent stimulator for hyaluronan production in DA SMCs [2], we investigated whether or not GH altered hyaluronan production in DA SMCs. We found that GH had no effect on hyaluronan production in DA SMCs (data not shown).

Effect of GH on tissue-specific cytoskeletal genes in the DA and the aorta

Our DNA array analyses revealed that the expression of cytoskeletal genes was markedly different between the DA and the aorta. Because GH is known to regulate cytoskeletal organization [7], we examined whether or not GH affected such a tissue-specific expression of cytoskeletal genes in DA SMCs. We found that GH decreased the expression of DA-dominant cytoskeletal genes such as desmin, Fhl2, Actg2, and Myh11 in DA SMCs (Fig. 4a–d). Among the aorta-dominant sarcomere genes, we also found that GH decreased the expression of Myl2 and Tnnt2 mRNAs, increased the expression of Tnni3 mRNA, and exhibited no change in Myh7, Actc1, and Tnnc2 mRNAs (Fig. 5).

Because GH is known to inhibit the expression of skeletal muscle-specific proteins in a dose-dependent manner in satellite cells [8], we examined the effect of GH on the expression of smooth muscle-specific genes. We found that GH significantly decreased the expression of SM1, SM2, SM22, and h-caldesmon mRNAs, whereas GH did not

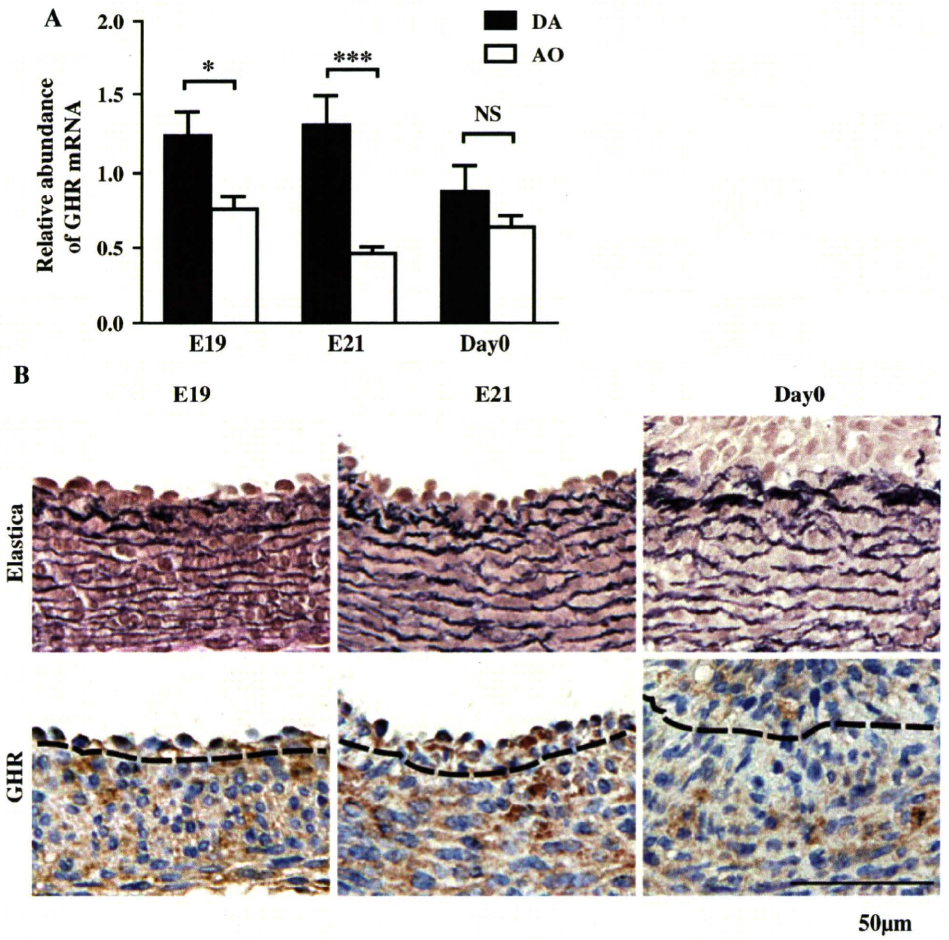

Fig. 2 Expression of GHR mRNA and protein in rat DA. **a** Quantitative RT-PCR analyses of GHR. The expression level of GHR mRNA was maximal at E19 and E21 in the DA ($n = 6$–8). **b** Immunohistological analysis of GHR protein in the rat DA at E19, E21, and Day0. GHR was detected in a *brown color*. Dark blue stain was counterstained with Mayer's hematoxylin. *Scale bars* 50 mm. $*p < 0.05$, $***p < 0.001$. Data are expressed as means ± SEM. *E19* Embryonic day 19, *E21* embryonic day 21, *Day0* at birth, *DA* ductus arteriosus, *AO* aorta, *GHR* growth hormone receptor, *NS* not significant

change the expression of SMemb mRNA (Fig. 6a–e). We also found that GH decreased the expression of myocardin mRNA (Fig. 6f), a transcriptional factor, which is sufficient for a smooth muscle-like contractile phenotype. To investigate whether the effect of GH on the expression of cytoskeletal genes is found in aortic SMCs, we also did the same experiment using SMCs from the rat aorta at e21. We also found a similar effect of GH on the expression of cytoskeletal genes in cultured rat aortic SMCs (Supplemental data 4, 5, and 6).

GH promoted intimal thickening of immature rat DA explants

To examine to what extent GH contributes to the intimal thickening of the DA, we administrated GH into the premature vessel explants containing the DA, the aorta, and the main pulmonary artery from fetuses at e19 (Fig. 7). We found that GH significantly promoted intimal thickening of the DA, but not the aorta when compared with the control (Fig. 7). It should be noted that the effect of GH on the intimal thickening was greater in the DA than in the aorta.

Discussion

Our microarray analyses uncovered gene expression profiles of the DA distinct from those of the aorta during fetal development. These gene expression profiles are considered to be the primary determinant of the different functional and morphological characteristics of the DA from the adjacent arteries. In fact, several unexpected genes that are known to be involved in tissue differentiation were identified as having a DA-dominant expression pattern. It is of note that among them GHR exhibited the highest difference in expression between the rat developing DA and the adjacent aorta. Although the expression levels of GH mRNA were slightly higher in the aorta than in the DA at e21, the difference did not reach statistical significance. We think that total GH-GHR signals are higher in the DA than in the aorta due to the predominant expression of GHR in the DA during gestation. Accordingly, we hypothesized that GH stimulation via GHR may be involved in DA remodeling and that it may play a role in the specification of the DA from other arteries. During gestation, the serum GH concentration of fetuses increased gradually as

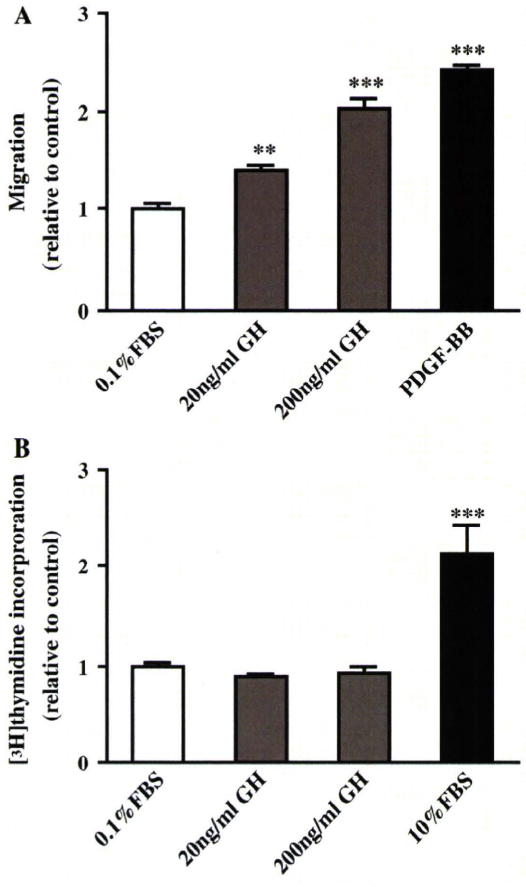

Fig. 3 GH promoted DA SMC migration, but not proliferation. **a** Effects of growth hormone (GH) stimulation on DA SMC migration. DA SMC migration was significantly increased in the presence of GH at a concentration of 20 or 200 ng/ml ($n = 6$). PDGF-BB at a concentration of 10 ng/ml was used as a positive control. **b** The effect of GH on proliferation of rat DA SMCs. GH did not promote cell proliferation in DA SMCs ($n = 6$–8); 10% FBS was used as a positive control. $^{**}p < 0.01$,$^{***}p < 0.001$ versus 0.1% FBS. Data are expressed as means ± SEM. *FBS* Fetal bovine serum

pregnancy advanced and declined before parturition in many species [9–11]. In rodents, the fetal pituitary gland starts to secret GH from e15, whereas many tissues, including vascular endothelial and SMCs, locally produce GH beginning in relatively early embryogenesis [12]. Even though the level of serum GH in a fetus is almost comparable to or slightly less than that in an adolescenct [9–11], GH has been regarded as of little functional significance in fetal growth [13]. A growing body of evidence, however, has revealed the importance of GH in tissue differentiation during fetal development. First, many fetal tissues, including vascular endothelium and smooth muscle, express GHR [14, 15]. Therefore, GH likely activates an intracellular signal pathway through GHR in fetuses. Second, a considerable number of studies have demonstrated that fetal tissues indeed respond to GH in vitro [12, 16], which was observed in the present study. Third, GHR knockout mice exhibit functional and morphological changes in both heart and vasculature [17]. These results led us to explore the role of GH in DA development, especially in its vascular remodeling.

Numerous previous studies have demonstrated that GH plays a role in angiogenesis [18] and that GH deficiency or excess increases the risk of cardiovascular morbidity and mortality [19, 20]. However, the role of GH in the vascular remodeling of the developmental arteries has not yet been precisely evaluated. The present study revealed that GH promoted the migration of DA SMCs and then intimal cushion formation in DA explants. In terms of the effect of GH on SMC migration, data from previous studies are very limited [21–23]. Although the precise mechanism still has not been investigated, it can be assumed that the different responses to GH in various cell types are dependent on the GHR expression levels.

Intimal thickness is a hallmark of physiological vascular remodeling of the DA during late gestation [2]. Although the present study demonstrated that GH promotes intimal cushion formation of the ex vivo DA explants, previous clinical studies have shown that the effect of GH on pathological intimal thickness is equivocal. Increases in the carotid intimal media thickness were observed in patients with acromegaly [24]. In contrast, patients with either childhood- or adulthood-onset GH deficiency also exhibited increased intima-media thickness and endothelial dysfunction [19, 25]. Therefore, adequate levels of GH could be important to maintain normal morphology of mature arteries. The present study indicates that GH in the culture media at a concentration of 200 ng/ml is sufficient to promote the physiological intimal cushion formation of the DA through increasing SMC migration.

It is known that the differentiation of DA SMCs precedes that of other arteries [26, 27]. Nevertheless, we were surprised by the considerable number of cardiac-type sarcomere genes expressed in the fetal DA, although it was much less than that in the aorta. The present data suggest that prior to complete differentiation, vascular SMCs may retain a high degree of plasticity, which allows them to modulate their phenotype [28]. Interestingly, through the in vitro experiment, we found that the effect of GH on the expression of the cytoskeletal genes was not always consistent with the tissue-dominant expression patterns that were identified by DNA microarray analysis. Therefore, factor(s) other than GH may determine the tissue-specific expression pattern of cytoskeletal genes in the DA and the aorta.

More importantly, we found that GH downregulated the genes involved in a smooth muscle-like contractile phenotype. Consistent with the result, we also found that GH downregulated myocardin mRNA, which is sufficient for a smooth muscle-like contractile phenotype [28]. In addition

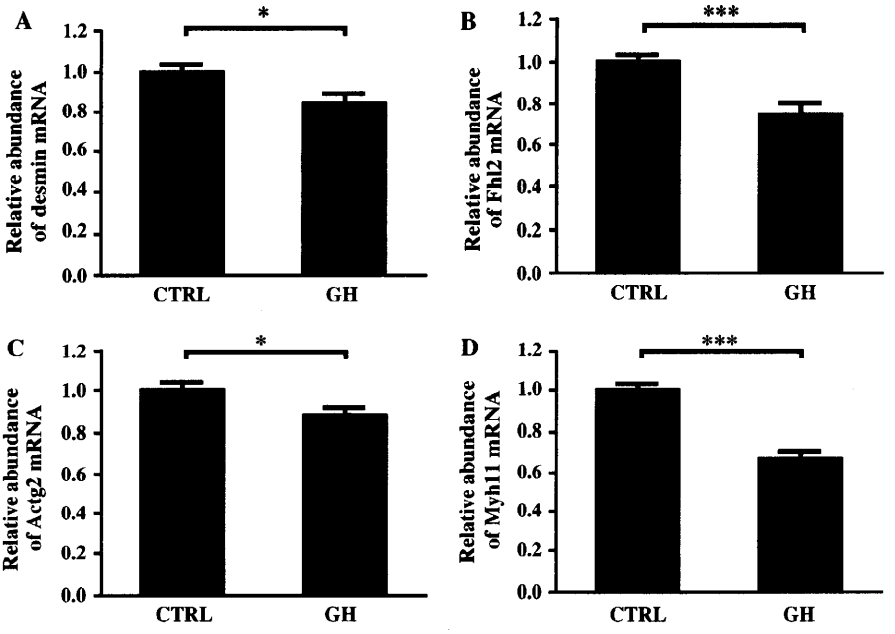

Fig. 4 Effect of GH on the cytoskeletal genes and smooth muscle-specific genes in DA SMCs. **a** Desmin, **b** Fhl2, **c** Actg2, **d** Myh11. ($n = 15$). $*p < 0.05$, $***p < 0.001$. Data are expressed as means ± SEM. *GH* Growth hormone, *CTRL* control, *DA SMC* ductus arteriosus smooth muscle cell, *NS* not significant

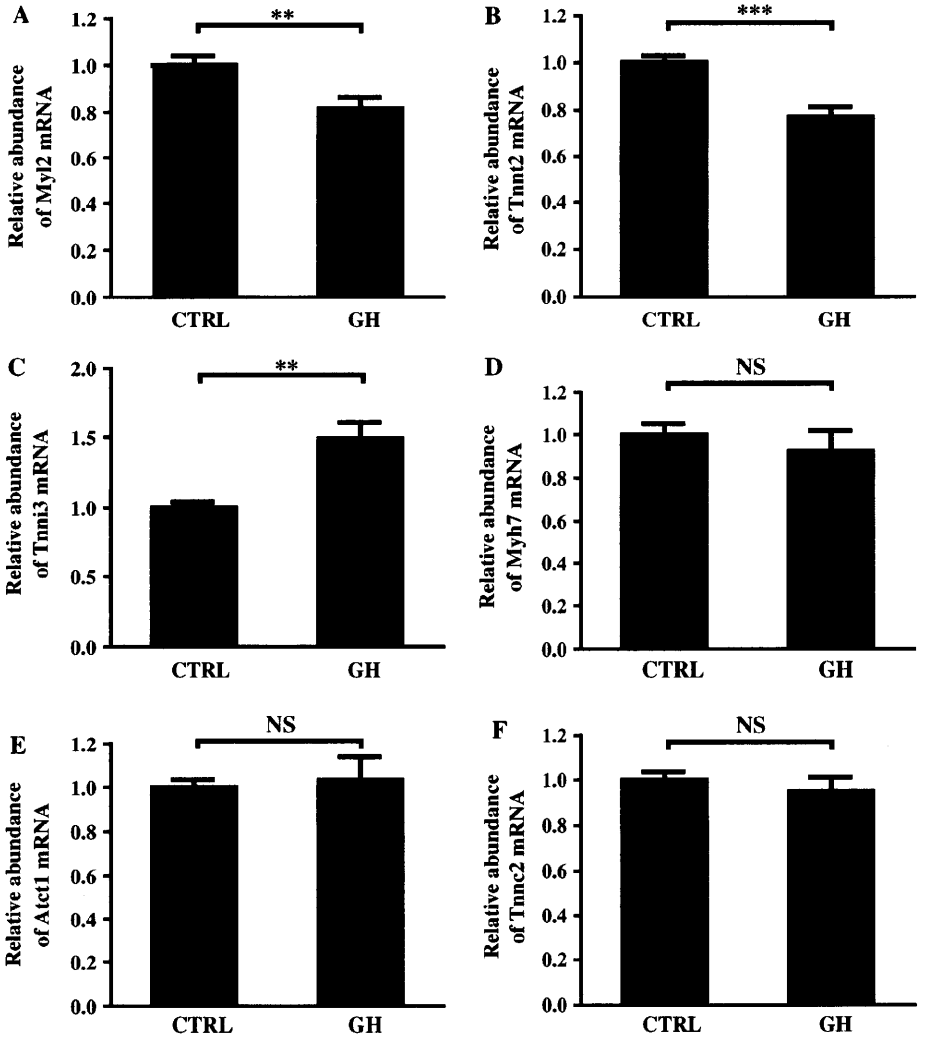

Fig. 5 Effect of GH on the expression of the aorta-dominant sarcomere genes in DA SMCs. **a** Myl2, **b** Tnnt2, **c** Tnni3, **d** Myh7, **e** Actc1, and **f** Tnnc2. ($n = 15$). $**p < 0.01$, $***p < 0.001$. Data are expressed as means ± SEM. *GH* Growth hormone, *CTRL* control, *DA SMC* ductus arteriosus smooth muscle cell, *NS* not significant

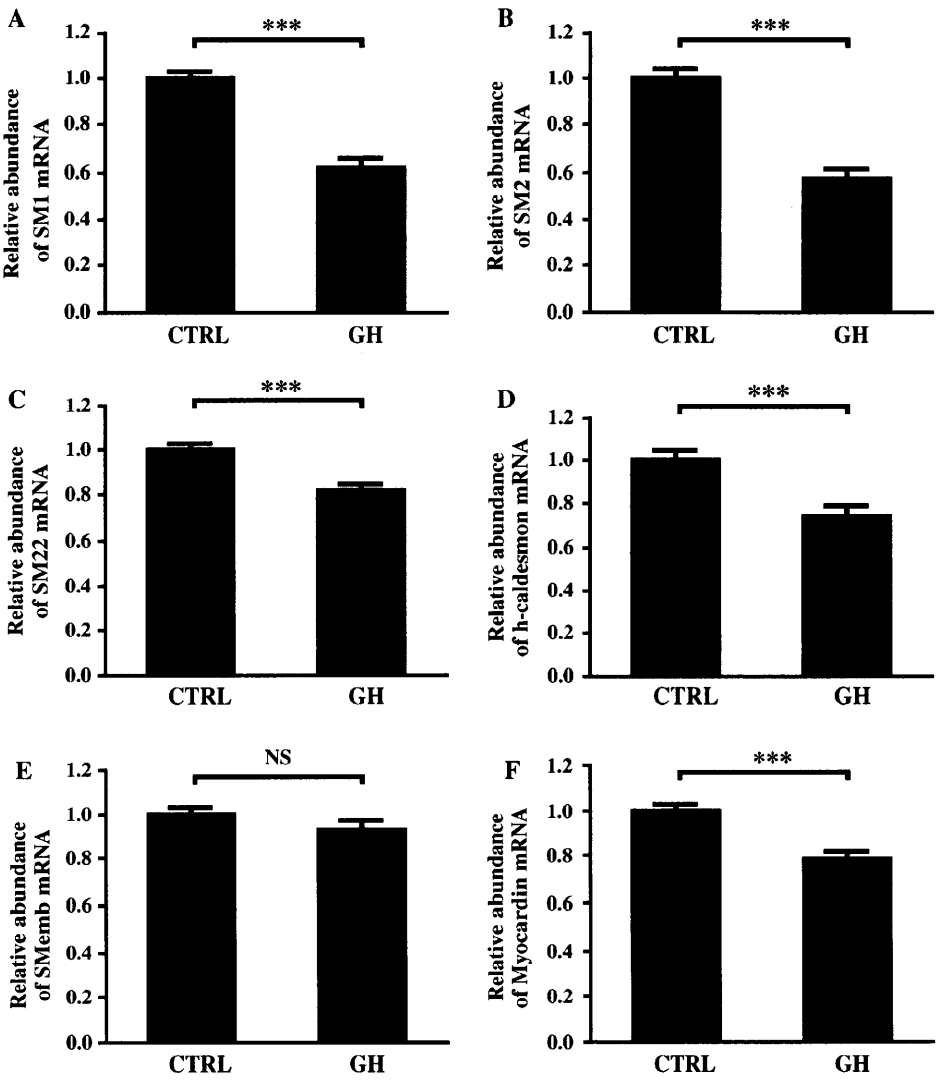

Fig. 6 Effect of GH on the cytoskeletal genes and smooth muscle-specific genes in DA SMCs. **a** SM1, **b** SM2, **c** SM22, **d** h-caldesmon, **e** SMemb, **f** Myocardin. ($n = 15$). $^{*}p < 0.05$, $^{***}p < 0.001$. Data are expressed as means ± SEM. *GH* Growth hormone, *CTRL* control, *DA SMC* ductus arteriosus smooth muscle cell, *NS* not significant

to this observation, Halevy et al. [8] demonstrated that GH inhibited the gene expression of myogenin and the expression of skeletal muscle-specific proteins in a dose-dependent manner in satellite cells. These data suggested that during muscle differentiation, GH inhibited the muscle-specific differentiation at its final stage to retain its synthetic phenotype. We propose that DA SMCs consist of distinct types that depend on their localization. During the progression of intimal cushion formation, DA SMCs in the inner layer are a synthetic phenotype that is highly proliferative and can migrate easily. The GH-GHR signal helps these cells remain a synthetic phenotype. Further studies are required to prove this idea.

Although the present microarray analyses uncovered distinct gene expression profiles of the DA from those of the aorta, several gene profiles are different from a previous report demonstrating the transcriptional profiles between the rat DA and the aorta of premature fetuses and neonates using the same DNA microarray plates we used [3]. For example, Costa et al. demonstrated that Myl2 and Myh7 are predominantly expressed in the rat aorta at e19, but our data showed the opposite result. In addition, the tissue-specific genes that we identified overlap very little with their findings. We do not have a reasonable explanation for this discrepancy. It should be noted that the present study identified several expected genes that are known to be predominantly expressed in the DA, such as prostaglandin E receptor 4, endothelin-1, and Kcnj8 (potassium inwardly rectifying channel, subfamily J, member 8). In contrast, Costa et al. did not identify this expected DA-dominant gene in the data from their microarray analysis. Furthermore, we also confirmed by quantitative RT-PCR analysis that, using different sets of RNA samples, the expression of several DA-dominant genes was higher in the DA than in the aorta. Therefore, we are confident that we provided

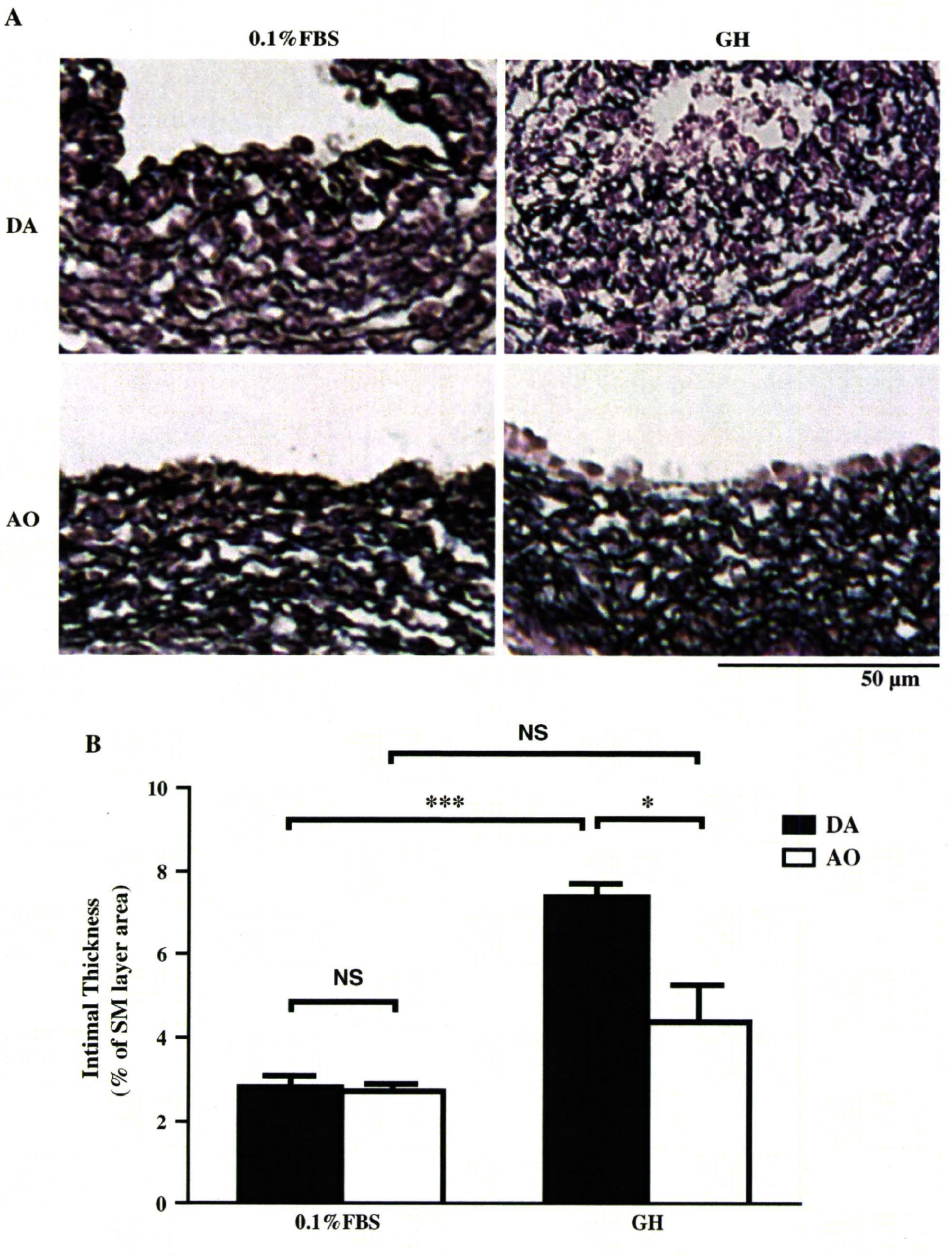

Fig. 7 Effects of GH-mediated intimal thickening of immature rat DA and aorta explants. **a** Elastica staining of the DA and the aorta. GH at a concentration of 200 ng/ml. *Scale bars* 50 μm. **b** GH significantly promoted intimal thickening of the DA, but not the aorta. ($n = 4$–6). $^{*}p < 0.05$,$^{***}p < 0.001$. Data are expressed as means ± SEM. *DA* Ductus arteriosus, *AO* aorta, *GH* growth hormone, *NS* not significant

reliable data regarding the transcriptional profiles of the developing rat DA.

In conclusion, our study highlighted the distinct transcriptional profiles of the DA. In addition to the expected genes, microarray analysis revealed many genes whose roles were previously unrecognized in the DA. Among them, we found that the GH-GHR signal plays a role in vascular remodeling of the DA by promoting migration of SMCs and the subsequent formation of intimal thickness and regulating the expression of cytoskeletal genes. Although further studies are needed to identify the role of other genes in the DA, our data provide a basis for understanding the molecular mechanisms underlying the differentiation and remodeling of the DA and for inventing the novel targets that regulate the contraction of the DA in affected children.

Acknowledgments This work was supported by grants from the Ministry of Health Labor and Welfare (Y.I.), the Ministry of Education, Culture, Sports, Science, and Technology of Japan (Y.I., U.Y., S.M.), the Foundation for Growth Science (S.M.), the Yokohama Foundation for Advanced Medical Science (U.Y., S.M.), the 'High-Tech Research Center' Project for Private Universities: MEXT (S.M.), a Waseda University Grant for Special Research Projects (Q.J.), the Vehicle Racing Commemorative Foundation (S.M.), Miyata Cardiology Research Promotion Funds (U.Y., S.M.), Takeda Science Foundation (Y.I., U.Y., S.M.), the Japan Heart Foundation Research Grant (U.Y.), the Kowa Life Science Foundation (U.Y.),

the Sumitomo Foundation (U.Y), Japan Cardiovascular Research Foundation (S.M.), Mochida Memorial Foundation for Medical and Pharmaceutical Research (U.Y.) and the Uehara Memorial Foundation (U.Y.).

References

1. Smith GC (1998) The pharmacology of the ductus arteriosus. Pharmacol Rev 50:35–58
2. Yokoyama U, Minamisawa S, Quan H, Ghatak S, Akaike T, Segi-Nishida E, Iwasaki S, Iwamoto M, Misra S, Tamura K, Hori H, Yokota S, Toole BP, Sugimoto Y, Ishikawa Y (2006) Chronic activation of the prostaglandin receptor EP4 promotes hyaluronan-mediated neointimal formation in the ductus arteriosus. J Clin Invest 116:3026–3034
3. Costa M, Barogi S, Socci ND, Angeloni D, Maffei M, Baragatti B, Chiellini C, Grasso E, Coceani F (2006) Gene expression in ductus arteriosus and aorta: comparison of birth and oxygen effects. Physiol Genomics 25:250–262
4. Yokoyama U, Sato Y, Akaike T, Ishida S, Sawada J, Nagao T, Quan H, Jin M, Iwamoto M, Yokota S, Ishikawa Y, Minamisawa S (2007) Maternal vitamin A alters gene profiles and structural maturation of the rat ductus arteriosus. Physiol Genomics 31:139–157
5. Akaike T, Jin MH, Yokoyama U, Izumi-Nakaseko H, Jiao Q, Iwasaki S, Iwamoto M, Nishimaki S, Sato M, Yokota S, Kamiya Y, Adachi-Akahane S, Ishikawa Y, Minamisawa S (2009) T-type Ca2+ channels promote oxygenation-induced closure of the rat ductus arteriosus not only by vasoconstriction but also by neointima formation. J Biol Chem 284:24025–24034
6. Yokoyama U, Minamisawa S, Katayama A, Tang T, Suzuki S, Iwatsubo K, Iwasaki S, Kurotani R, Okumura S, Sato M, Yokota S, Hammond HK, Ishikawa Y (2010) Differential regulation of vascular tone and remodeling via stimulation of type 2 and type 6 adenylyl cyclases in the ductus arteriosus. Circ Res 106:1882–1892
7. Florini JR, Ewton DZ, Coolican SA (1996) Growth hormone and the insulin-like growth factor system in myogenesis. Endocr Rev 17:481–517
8. Halevy O, Hodik V, Mett A (1996) The effects of growth hormone on avian skeletal muscle satellite cell proliferation and differentiation. Gen Comp Endocrinol 101:43–52
9. Kishi K, Hirashiba M, Hasegawa Y (1991) Gestational profiles of rat placental lactogen-II (rPL-II) and growth hormone (GH) in maternal and fetal serum, amniotic fluid, and placental tissue. Endocrinol Jpn 38:589–595
10. Bassett JM, Thorburn GD, Wallace AL (1970) The plasma growth hormone concentration of the foetal lamb. J Endocrinol 48:251–263
11. Kaplan SL, Grumbach MM, Shepard TH (1972) The ontogenesis of human fetal hormones I. Growth hormone and insulin. J Clin Invest 51:3080–3093
12. Waters MJ, Kaye PL (2002) The role of growth hormone in fetal development. Growth Horm IGF Res 12:137–146
13. Gluckman PD, Grumbach MM, Kaplan SL (1981) The neuroendocrine regulation and function of growth hormone and prolactin in the mammalian fetus. Endocr Rev 2:363–395
14. Garcia-Aragon J, Lobie PE, Muscat GE, Gobius KS, Norstedt G, Waters MJ (1992) Prenatal expression of the growth hormone (GH) receptor/binding protein in the rat: a role for GH in embryonic and fetal development? Development 114:869–876
15. Beyea JA, Olson DM, Vandergriend RA, Harvey S (2005) Expression of growth hormone and its receptor in the lungs of embryonic chicks. Cell Tissue Res 322:379–392
16. Giustina A, Mazziotti G, Canalis E (2008) Growth hormone, insulin-like growth factors, and the skeleton. Endocr Rev 29:535–559
17. Egecioglu E, Andersson IJ, Bollano E, Palsdottir V, Gabrielsson BG, Kopchick JJ, Skott O, Bie P, Isgaard J, Bohlooly YM, Bergstrom G, Wickman A (2007) Growth hormone receptor deficiency in mice results in reduced systolic blood pressure and plasma renin, increased aortic eNOS expression, and altered cardiovascular structure and function. Am J Physiol Endocrinol Metab 292:E1418–E1425
18. Lincoln DT, Singal PK, Al-Banaw A (2007) Growth hormone in vascular pathology: neovascularization and expression of receptors is associated with cellular proliferation. Anticancer Res 27:4201–4218
19. Klibanski A (2003) Growth hormone and cardiovascular risk markers. Growth Horm IGF Res 13(Suppl A):S109–S115
20. Colao A (2008) The GH-IGF-I axis and the cardiovascular system: clinical implications. Clin Endocrinol (Oxf) 69:347–358
21. Schultz K, Rasmussen LM, Ledet T (2005) Expression levels and functional aspects of the hyaluronan receptor CD44. Effects of insulin, glucose, IGF-I, or growth hormone on human arterial smooth muscle cells. Metabolism 54:287–295
22. Ikeo S, Yamauchi K, Shigematsu S, Nakajima K, Aizawa T, Hashizume K (2001) Differential effects of growth hormone and insulin-like growth factor I on human endothelial cell migration. Am J Physiol Cell Physiol 280:C1255–C1261
23. Lee SW, Kim SH, Kim JY, Lee Y (2010) The effect of growth hormone on fibroblast proliferation and keratinocyte migration. J Plast Reconstr Aesthet Surg 63:e364–e369
24. Colao A, Spiezia S, Cerbone G, Pivonello R, Marzullo P, Ferone D, Di Somma C, Assanti AP, Lombardi G (2001) Increased arterial intima-media thickness by B-M mode echodoppler ultrasonography in acromegaly. Clin Endocrinol (Oxf) 54:515–524
25. Pfeifer M, Verhovec R, Zizek B, Prezelj J, Poredos P, Clayton RN (1999) Growth hormone (GH) treatment reverses early atherosclerotic changes in GH-deficient adults. J Clin Endocrinol Metab 84:453–457
26. Kim HS, Aikawa M, Kimura K, Kuro-o M, Nakahara K, Suzuki T, Katoh H, Okamoto E, Yazaki Y, Nagai R (1993) Ductus arteriosus. Advanced differentiation of smooth muscle cells demonstrated by myosin heavy chain isoform expression in rabbits. Circulation 88:1804–1810
27. Colbert MC, Kirby ML, Robbins J (1996) Endogenous retinoic acid signaling colocalizes with advanced expression of the adult smooth muscle myosin heavy chain isoform during development of the ductus arteriosus. Circ Res 78:790–798
28. Kumar MS, Owens GK (2003) Combinatorial control of smooth muscle-specific gene expression. Arterioscler Thromb Vasc Biol 23:737–747

Heterologous down-regulation of angiotensin type 1 receptors by purinergic $P2Y_2$ receptor stimulation through S-nitrosylation of NF-κB

Motohiro Nishida[a], Mariko Ogushi[a], Reiko Suda[a], Miyuki Toyotaka[a], Shota Saiki[a], Naoyuki Kitajima[a], Michio Nakaya[a], Kyeong-Man Kim[b], Tomomi Ide[c], Yoji Sato[d], Kazuhide Inoue[e], and Hitoshi Kurose[a,1]

[a]Department of Pharmacology and Toxicology, Graduate School of Pharmaceutical Sciences, Kyushu University, Fukuoka 812-8582, Japan; [b]Department of Pharmacology, College of Pharmacy, Chonnam National University, Gwang-Ju 500-757 Korea; [c]Department of Cardiovascular Medicine, Graduate School of Medical Sciences, Kyushu University, Fukuoka 812-8582, Japan; [d]Division of Cellular and Gene Therapy Products, National Institute of Health Sciences, Tokyo 158-8501, Japan; and [e]Department of Molecular and System Pharmacology, Graduate School of Pharmaceutical Sciences, Kyushu University, Fukuoka 812-8582, Japan

Edited by Robert J. Lefkowitz, Duke University Medical Center/Howard Hughes Medical Institute, Durham, NC, and approved March 3, 2011 (received for review November 24, 2010)

Cross-talk between G protein-coupled receptor (GPCR) signaling pathways serves to fine tune cellular responsiveness by neurohumoral factors. Accumulating evidence has implicated nitric oxide (NO)-based signaling downstream of GPCRs, but the molecular details are unknown. Here, we show that adenosine triphosphate (ATP) decreases angiotensin type 1 receptor (AT_1R) density through NO-mediated S-nitrosylation of nuclear factor κB (NF-κB) in rat cardiac fibroblasts. Stimulation of purinergic $P2Y_2$ receptor by ATP increased expression of inducible NO synthase (iNOS) through activation of nuclear factor of activated T cells, NFATc1 and NFATc3. The ATP-induced iNOS interacted with p65 subunit of NF-κB in the cytosol through flavin-binding domain, which was indispensable for the locally generated NO-mediated S-nitrosylation of p65 at Cys38. β-Arrestins anchored the formation of p65/IκBα/β-arrestins/iNOS quaternary complex. The S-nitrosylated p65 resulted in decreases in NF-κB transcriptional activity and AT_1R density. In pressure-overloaded mouse hearts, ATP released from cardiomyocytes led to decrease in AT_1R density through iNOS-mediated S-nitrosylation of p65. These results show a unique regulatory mechanism of heterologous regulation of GPCRs in which cysteine modification of transcriptional factor rather than protein phosphorylation plays essential roles.

G protein-coupled receptors (GPCRs) are the largest family of cell-surface receptors, which play a critical role in regulating multiple physiological functions (1, 2). Abnormal activation or up-regulation of GPCRs is a major cause of various diseases (3), and about 40% of drugs that are widely used for therapeutic treatment all over the world may directly or indirectly target GPCRs.

An important adaptive response of the cell against multiple extracellular stimuli is receptor desensitization, which refers to the reduction of receptor responsiveness despite continuing agonist stimulation. GPCRs have developed elaborate means of turning off signal (4). One mechanism for desensitization is receptor down-regulation, which refers to the net loss of receptors from the cell by a decrease in receptor synthesis, a destabilization of receptor mRNA, or an increase in receptor degradation (4, 5).

Two major patterns of down-regulation have been characterized; homologous (or agonist specific) down-regulation and heterologous (or agonist nonspecific) down-regulation (6). The homologous down-regulation indicates that stimulation of one GPCR over time by the agonist reduces expression levels of the same GPCR, without substantial effect on other GPCRs present in the same cell. In contrast, heterologous down-regulation indicates that stimulation of one GPCR reduces expression levels of different GPCR. Although the molecular mechanism of homologous down-regulation has been well analyzed using β-adrenergic receptors (βARs) (4, 5), the mechanism(s) underlying heterologous down-regulation is largely unknown.

Angiotensin (Ang) II is a major bioactive polypeptide, and improper regulation of Ang II induces various cardiovascular diseases, including hypertension, cardiac hypertrophy, fibrosis, apoptosis, and arrhythmia (7). Most of known physiological and pathological effects of Ang II are mediated via the angiotensin type 1 receptor (AT_1R). In fact, aberrant expression of AT_1R has been shown to have pathophysiological relevance in cell culture, animal studies, and clinical interventional trials (8). Ang II decreases AT_1R expression level through destabilization of AT_1R mRNA (9), suggesting the involvement of homologous down-regulation processes. In addition, the expression of AT_1Rs could be regulated by various factors, including cytokines, growth factors, and reactive oxygen species (ROS). However, heterologous down-regulation of AT_1Rs through different GPCRs has not been reported.

It is well established that nitric oxide (NO) regulates a diverse array of signal transduction pathways, acting in significant part through the covalent modification of cysteine (Cys) thiols (S-nitrosylation) that are found at active or allosteric sites of proteins (10). Many GPCRs and their downstream signaling molecules could be modified by NO, including NMDA receptor (11), GPCR kinase 2 (12), β-arrestin (13), and G proteins (14, 15). Although exposure of excessive NO has been reported to decrease AT_1R density (16), the molecular details and its physiological significance are still unknown.

During the analysis of the roles of Ca^{2+} signaling in cardiac fibroblasts, we noticed that the pretreatment with adenosine triphosphate (ATP) selectively suppressed AT_1R-stimulated Ca^{2+} response. We have found that stimulation of $P2Y_2$ receptor with ATP down-regulates AT_1R signaling through expression of inducible NO synthase (iNOS) without nuclear factor κB (NF-κB) activation. Down-regulation of AT_1R requires functional interaction of NF-κB with iNOS, and the locally generated NO mediates cysteine modification (S-nitrosylation) of NF-κB, leading to suppression of AT_1R transcription rate.

Author contributions: M. Nishida designed research; M. Nishida, M.O., R.S., M.T., S.S., N.K., T.I., and Y.S. performed research; K.I. contributed new reagents/analytic tools; M. Nishida, M.O., R.S., M.T., S.S., M. Nakaya, and Y.S. analyzed data; and M. Nishida, K.-M.K., and H.K. wrote the paper.

The authors declare no conflict of interest.

This article is a PNAS Direct Submission.

[1]To whom correspondence should be addressed. E-mail: kurose@phar.kyushu-u.ac.jp.

This article contains supporting information online at www.pnas.org/lookup/suppl/doi:10.1073/pnas.1017640108/-/DCSupplemental.

Results

$P2Y_2$ Receptor Stimulation Selectively Down-Regulates AT_1R Signaling. In a normal heart, two-thirds of the cell population is composed of cardiac fibroblasts. Expression level of AT_1R in rat neonatal cardiac fibroblasts is more than fivefold higher than that in rat neonatal cardiomyocytes (65 ± 12 fmol/mg protein), and AT_1R signaling in cardiac fibroblasts has been implicated in the development of cardiac fibrosis (17). We have previously reported that treatment with Ang II increases activity of nuclear factor of activated T cells (NFAT), a Ca^{2+}-dependent transcriptional factor that is predominantly regulated by calcineurin, both in cardiac myocytes and fibroblasts (18, 19). Activation of NFAT has been implicated in the development of cardiac hypertrophy (20), but the role of NFAT in cardiac fibroblasts is fully unknown. Therefore, we first examined the relationship between NFAT activity and AT_1R signaling in cardiac fibroblasts. We found that treatment with ATP more potently increased NFAT activity than Ang II, the endogenous ligand of G_qPCR (Fig. 1 *A* and *B*). Purinergic receptors are classified into two families, P2X and P2Y (21). P2X receptors are ligand-gated channels. P2Y receptors are G protein-coupled receptors, and divided into eight subtypes. Purinergic signaling has been implicated in inflammatory responses of various systems (22, 23), and we have also reported that extracellular nucleotides trigger pressure overload-induced cardiac fibrosis in mice (24). The ATP-induced increases in intracellular Ca^{2+} concentration ($[Ca^{2+}]_i$) and NFAT activity were completely suppressed by the inhibition of phospholipase C (PLC) and knockdown of $P2Y_2$ receptor ($P2Y_2R$), but not by inhibition of $P2Y_1R$ and $P2Y_6R$ (Fig. S1). These results suggest that $P2Y_2R$ predominantly regulates ATP-induced activation of Ca^{2+} signaling in rat cardiac fibroblasts.

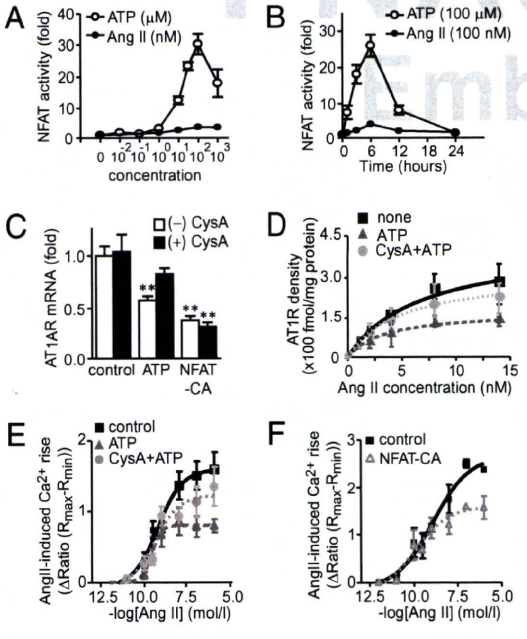

Fig. 1. ATP decreases AT_1R density through NFAT activation. (*A*) Concentration-dependent NFAT activation induced by ATP and Ang II in rat neonatal cardiac fibroblasts. Cells were treated with indicated concentration of ATP or Ang II for 6 h. (*B*) Time courses of NFAT activation induced by ATP and Ang II. (*C*) Changes in $AT_{1A}R$ mRNA expression levels by the treatment with ATP (100 μM) for 24 h or overexpression of NFAT-CA in the presence or absence of CysA (100 ng/mL). Cells were treated with CysA 10 min before ATP stimulation. (*D*) Changes in AT_1R density induced by ATP (100 μM) for 24 h with or without CysA (n = 4–6). (*E*) Peak increases in $[Ca^{2+}]_i$ induced by Ang II stimulation in ATP-treated or ATP/CysA-treated cardiac fibroblasts. Cells were treated with CysA (100 ng/mL) 10 min before stimulation of ATP (100 μM) for 24 h. (*F*) Peak $[Ca^{2+}]_i$ increases induced by Ang II in LacZ (control)- and NFAT-CA-expressing cardiac fibroblasts. Cells were infected with Ad-LacZ or Ad-NFAT-CA for 48 h (n = 63–99). $^{**}P < 0.01$.

The treatment with ATP for 24 h resulted in a decrease in expression levels of AT_1R mRNA and protein (Fig. 1 *C* and *D*), which was abolished by cyclosporine A, a specific calcineurin inhibitor. In addition, expression of Cain, a specific inhibitory peptide of calcineurin (25), also canceled the ATP-induced decrease in AT_1R density and AT_1R-induced signaling (Fig. S2 *A–C*). Expression of constitutively active mutant of NFAT4 (NFAT-CA) inhibited AT_1R mRNA expression (Fig. 1*C*), indicating that calcineurin-NFAT signaling mediates AT_1R down-regulation. As AT_1R couples with G_q family proteins, the Ang II-induced transient increase in $[Ca^{2+}]_i$ was measured as an index of the magnitude of AT_1R signaling. Pretreatment with ATP or overexpression of NFAT-CA significantly decreased the Ang II-induced maximal $[Ca^{2+}]_i$ increases without changing EC_{50} values (Fig. 1 *E* and *F*). There are four NF-AT isoforms responsive to increase in $[Ca^{2+}]_i$ (26). Among them, NFATc1 participates in cardiac valve development and NFATc3 participates in the development of cardiac hypertrophy. Treatment of cardiac fibroblast with ATP induced nuclear translocation of NFATc1 and NFATc3, but not NFATc2 (Fig. S2 *D* and *E*). We could not detect the expression of NFATc4 proteins. These results suggest that stimulation of G_q-coupled $P2Y_2$ receptor by ATP induces heterologous down-regulation of G_q-coupled AT_1R through activation of NFATc1 and NFATc3 in rat cardiac fibroblasts. Although $P2Y_2R$ can be stimulated not only by ATP but also by ADP and UTP (21), ATP maximally increased NFAT activity and decreased AT_1R signaling (Fig. S3). However, endothelin-1 and bradykinin, which signal through G_q (27), failed to imitate ATP both in NFAT activation and inhibition of G_q signaling, suggesting that the ATP-mediated suppression of AT_1R signaling is likely to correlate with its potential to increase NFAT activity. Furthermore, pretreatment with Ang II did not affect the ATP-induced Ca^{2+} response (Fig.S3 *C* and *D*), suggesting that ATP specifically induces heterologous down-regulation of AT_1R signaling but not vice versa.

ATP Decreases AT_1R Density Through iNOS Expression. We next examined the mechanism of AT_1R down-regulation by NFAT activation. Because the mRNA stability of AT_1R was not decreased by ATP treatment (Fig. S3*E*), its effects on the AT_1R transcription rate were further studied. NF-κB has been reported to participate in AT_1R up-regulation induced by cytokines or bacterial toxin (28, 29), and inhibition of NF-κB significantly suppressed AT_1R transcription rate and AT_1R density (Fig. S4). Thus, basal activity of AT_1R transcription may be mainly regulated by NF-κB. In addition, NO has been reported to decrease NF-κB and AT_1R transcription (16). Thus, NO may mediate ATP-induced AT_1R down-regulation. Treatment with ATP induced a time-dependent decrease in expression of luciferase from AT_1R promoter, as well as a decrease in NF-κB–dependent luciferase activity (Fig. 2*A*). The ATP-induced suppression of AT_1R transcription rate was abolished by N(G)-nitro-L-arginine methyl ester (L-NAME) or *N*-(3-(aminomethyl)benzyl)acetamidine (1400W), a specific inhibitor of iNOS (Fig. 2*B*). Treatment with 1400W canceled the ATP-induced decrease in AT_1R density and suppression of AT_1R-stimulated Ca^{2+} response (Fig. 2 *C–E*). In addition, knockdown of iNOS, but not endothelial NOS (eNOS), abolished the ATP-induced suppression of Ca^{2+} response by AT_1R stimulation (Fig. 2*F*), suggesting that iNOS mediates ATP-induced AT_1R down-regulation. It is generally accepted that NF-κB predominantly regulates the expression level of iNOS proteins (30). However, it has also been reported that iNOS proteins are induced by the constitutive activation of calcineurin-NFAT signaling in cardiomyocytes (31). In accordance with this, the expression of a constitutively active mutant

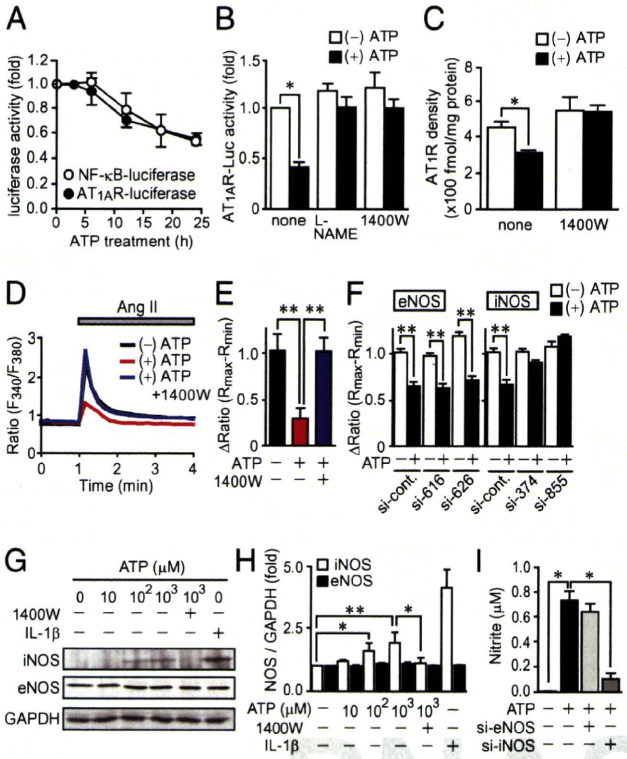

Fig. 2. iNOS mediates ATP-induced AT_1R down-regulation. (*A*) Time-dependent suppression of NF-κB-dependent and $rAT_{1A}R$ promoter-dependent luciferase activities induced by ATP (100 μM). (*B*) Effects of iNOS inhibitors on the ATP-induced decrease in $rAT_{1A}R$ promoter activity. Cells were treated with L-NAME (100 μM) or 1400W (10 μM) 10 min before sitmulation with ATP (100 μM) for 24 h. (*C*) Effects of 1400W on the ATP-induced decrease in AT_1R protein expression (n = 3–5). (*D*) Time courses of AT_1R-stimulated increases in $[Ca^{2+}]_i$ in cardiac fibroblasts pretreated with ATP or ATP and 1400W. (*E*) Peak increases in $[Ca^{2+}]_i$ induced by Ang II (100 nM). Cells were treated with 1400W (10 μM) 10 min before sitmulation with ATP (100 μM) for 24 h. (*F*) Peak increases in $[Ca^{2+}]_i$ induced by Ang II in siRNA-transfected cardiac fibroblasts pretreated with or without ATP (100 μM) for 24 h. Cells were treated with ATP 48 h after transfection with siRNAs for eNOS and iNOS. (n = 42–78) (*G* and *H*) Changes in expressions of iNOS, eNOS and GAPDH proteins by the stimulation with ATP and IL-1β (1 ng/mL) for 24 h in the presence or absence of 1400W (10 μM). (*I*) Effects of siRNAs for eNOS or iNOS on the ATP-induced nitrite production. Cells were treated with ATP (100 μM) for 24 h. (n = 3). $^*P < 0.05$, $^{**}P < 0.01$.

of NFAT (NFAT-CA) decreased AT_1R-stimulated Ca^{2+} response, which was completely abolished by the treatment with L-NAME or 1400W (Fig. S5). ATP-stimulated increase of iNOS proteins was completely suppressed by 1400W (Fig. 2 *G* and *H*). In addition, ATP-induced NO production was completely suppressed by the knockdown of iNOS, but not eNOS (Fig. 2*I*). As ATP strongly induced NFAT activity, NFAT-dependent iNOS expression may mediate the ATP-induced down-regulation of AT_1R in cardiac fibroblasts.

Requirement of S-Nitrosylation of p65 for ATP-Induced AT_1R Down-Regulation. As the treatment with protein kinase G (PKG) inhibitor (KT5823) did not cancel the ATP-induced down-regulation of AT_1R signaling, and a cGMP analog (8-bromo-cGMP) did not induce AT_1R down-regulation (Fig. S5 *A* and *B*), NO may suppress AT_1R transcription in a cGMP-independent manner. S-nitrosylation has been recently recognized as a new NO-based but cGMP-independent signaling regulating several cardiovascular functions (10). Dimers of NF-κB proteins are composed of five transcriptional factors: p50, p52, p65, Rel, and RelB, which all share an N-terminal Rel homology domain (32). Among them, S-nitrosylation of p50 and p65 has been reported to participate in iNOS-induced decrease in NF-κB transcriptional activity (33, 34). We next examined whether S-nitrosylation participates in ATP-induced AT_1R down-regulation. It was reported that a conserved Cys within the DNA-binding site of the Rel homology domain is the site of S-nitrosylation (33). Thus, we constructed Cys mutants of p65 (p65-C38S) and p50 (p50-C62S) to examine which Cys is involved in ATP-induced AT_1R down-regulation. Overexpression of wild-type p65 (p65-WT) and p65-C38S enhanced the AT_1R-stimulated increases in $[Ca^{2+}]_i$, suggesting that transcriptional activity of p65 is not affected by substitution of Ser for Cys. The ATP-induced suppression of AT_1R signaling normally occurred in vector- and p65-WT–expressing cardiac fibroblasts but was completely abolished in p65-C38S–expressing cardiac fibroblasts (Fig. 3 *A* and *B*). Substitution of Ser for other eight Cys residues of p65 did not affect the ATP-induced suppression of AT_1R signaling (Fig. S6), suggesting that Cys38 of p65 participates in ATP-induced S-nitrosylation and AT_1R down-regulation. In contrast, expression of p50-C62S did not abolish the suppression of AT_1R signaling induced by ATP (Fig. 3 *C* and *D*). Although p50 essentially lacks transactivation domain (32), overexpression of p50-WT and p50-C62S enhanced the AT_1R-stimulated Ca^{2+} responses, suggesting that p50 does not mediate ATP-induced suppression of AT_1R signaling. It has been previously reported that phosphorylation of p65 at Ser468 reduces basal NF-κB activity (35). However, treatment with ATP did not increase the phosphorylation

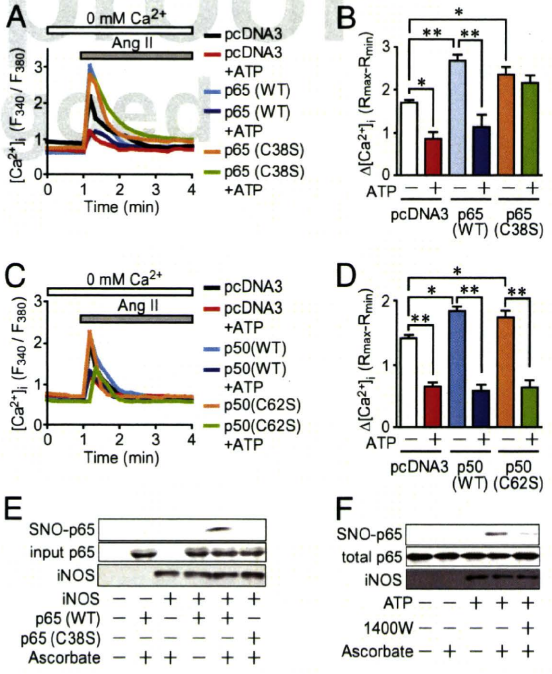

Fig. 3. S-nitrosylation of p65 mediates ATP-induced AT1R down-regulation. (*A*) Time courses of Ca^{2+} responses induced by Ang II (100 nM) in vector, p65 (WT) or p65 (C38S)-overexpressing cardiac fibroblasts. Cells were pretreated with ATP (100 μM) for 24 h. (*B*) Peak increases in $[Ca^{2+}]_i$ induced by Ang II (n = 41–68). (*C, D*) Time courses (*C*) and peak changes (*D*) of Ca^{2+} responses induced by Ang II in vector, p50 (WT) or p50 (C62S)-expressing fibroblasts (n = 44–72). (*E*) S-nitrosylation of Cys38 of p65 in p65 and iNOS-expressing HEK293 cells. Cell lysates were incubated with ascorbate (1 mM) for 1 h at 25 °C in the dark room. (*F*) S-nitrosylation of p65 and iNOS expression induced by ATP stimulation in cardiac fibroblasts. Cells were treated with 1400 W (10 μM) 10 min before stimulation with ATP (100 μM) for 24 h. Cell lysates were incubated with ascorbate (1 mM) for 1 h at 25 °C in the dark room (n = 3). $^*P < 0.05$, $^{**}P < 0.01$.

level of p65 at Ser468, and substitution of Ala for Ser468 did not affect the suppression of AT_1R-stimulated Ca^{2+} response induced by ATP (Fig. S6 *D–F*). Thus, phosphorylation of p65 is not involved in ATP-induce AT_1R down-regulation. The expression of iNOS proteins induced S-nitrosylation of p65 at Cys38 in HEK293 cells (Fig. 3*E*), and the treatment of cardiac fibroblasts with ATP induced S-nitrosylation of p65 in an iNOS-dependent manner (Fig. 3*F*). These results suggest that S-nitrosylation of p65 at Cys38 participates in the ATP-induced AT_1R down-regulation in cardiac fibroblasts.

Requirement of the Interaction Between iNOS and p65 for ATP-Induced AT_1R Down-Regulation. The extent of iNOS induction by ATP was smaller than that by IL-1β, a potent activator of NF-κB signaling (Fig. 2 *G* and *H*). This apparent discrepancy may be explained by the differences in the colocalization between p65 and iNOS, which is predominantly expressed in the cytosol (33), in ATP-, and IL-1β–treated cells. In iNOS- and p65-overexpressing HEK293 cells, both p65-WT and p65-C38S interacted with iNOS (Fig. 4*A*). In addition, iNOS induced by ATP, but not eNOS, interacted with p65 in rat cardiac fibroblasts, which was completely suppressed by cyclosporine A (Fig. 4*B*). Although cotreatment with S-nitrosoglutathione (GSNO) (1 mM) significantly enhanced ATP-induced S-nitrosylation of p65, GSNO did not affect the ATP-induced interaction between p65 and iNOS (Fig. S7). These results suggest that p65 associates with iNOS independently of Cys modification. In the resting condition, p65 was expressed both in the cytosol and nucleus, whereas iNOS was hardly detected in cardiac fibroblasts (Fig. 4*C*). Treatment with ATP induced expression of iNOS in the cytosol without affecting the subcellular localization of p65, resulting in colocalization of p65 and iNOS in the cytosol. In contrast, IL-1β markedly increased expression levels of iNOS and induced continuous translocation of p65 into the nucleus, resulting in little colocalization between p65 and iNOS. We next examined which domain of iNOS is required for the interaction with p65. As iNOS has N-terminal oxygenase domain and C-terminal reductase domain (36), and the C-terminal domain has flavin-binding domain and NADPH-binding domain, we constructed four fragments of iNOS (Fig. 4 *D* and *E*). In HEK293 cells expressing p65 and each iNOS fragment (Fr-I–Fr-IV), p65 was interacted with Fr-III only, which contains flavin-binding domain (Fig. 4*F*). Furthermore, expression of cardiac fibroblasts with Fr-III completely blocked the ATP-induced interaction of p65 with iNOS and suppression of AT_1R-stimulated Ca^{2+} response (Fig. 4 *G* and *H*). These results suggest that iNOS induced by ATP stimulation interacts with p65 in the cytosol through flavin-binding domain, which is required for S-nitrosylation of p65 and which decreases in its activity in rat cardiac fibroblasts.

Previous reports have clearly shown that β-arrestins associate with NOS and IκBα (13, 37–39). As the IκBα interacts with NF-κB p65 subunit, ATP may induce the formation of quaternary complex of iNOS/β-arrestin/IκBα/p65 in cardiac fibroblasts. To verify this hypothesis, we further examined whether knockdown of β-arrestin(s) cancels the ATP-induced p65-iNOS interaction. Knockdown of β-arrestin2 significantly suppressed the down-regulation of AT_1R signaling (Fig. S8). The β-arrestins were predominantly expressed in the cytosol of cardiac fibroblasts, and the ATP-induced colocalization of p65 with iNOS was diminished by β-arrestin2 knockdown. In addition, p65 actually interacted not only with iNOS, but also IκBα and β-arrestin2 in ATP-pretreated cardiac fibroblasts, which was diminished by β-arrestin2 knockdown. Although knockdown of β-arrestin1 also suppressed the p65-iNOS colocalization and down-regulation of AT_1R signaling induced by ATP pretreatment, the magnitude of suppression was smaller than that of β-arrestin2. These results

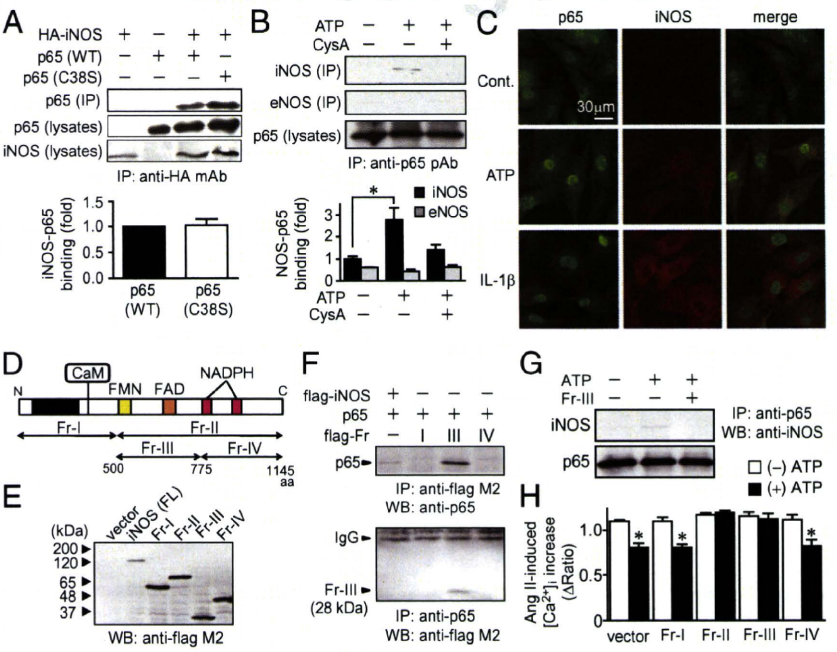

Fig. 4. ATP-induced iNOS interacts with p65. (*A*) Association of iNOS proteins with p65 (WT or C38S) in p65 and iNOS-expressing HEK293 cells. IP: immunoprecipitation, WB: Western blotting. HA-tagged iNOS proteins were immunoprecipitated with anti-HA antibody (IP), and combined p65 proteins were detected by Western blotting. Expression levels of p65 and iNOS were also confirmed using total cell lysates (lysates). (*B*) ATP stimulation-dependent interaction of p65 with iNOS in cardiac fibroblasts. Cells were treated with ATP (100 μM) for 24 h in the presence or absence of CysA (100 ng/mL). Native p65 proteins were immunoprecipitated with anti-p65 antibody (IP) (n = 3). (*C*) Localization of p65 and iNOS proteins in cardiac fibroblasts stimulated with ATP (100 μM) or IL-1β (1 ng/mL) for 24 h. (*D*) Structure of iNOS fragments (Fr-I – Fr-IV). (*E*) Expression of flag-tagged iNOS fragments. FL; full length. (*F*) Interaction of p65 with Fr-III. (*G*) Effects of Fr-III on the ATP-induced interaction of p65 with iNOS (n = 3). (*H*) Effects of iNOS fragments on the ATP-induced down-regulation of AT_1R signaling (n = 39–62). $^*P < 0.05$.

indicate that β-arrestins mediate the ATP-induced formation of quaternary complex of iNOS/β-arrestin/IκBα/p65 in the cytosol of cardiac fibroblasts. Although β-arrestins participate in GPCR-stimulated activation of extracellular signal-regulated kinase (ERK), treatment with ERK inhibitors (U0126 and PD98059) did not cancel the ATP-induced down-regulation of AT_1R signaling (Fig. S9). Thus, β-arrestins may participate in ATP-induced AT_1R down-regulation through anchoring the interaction between p65 and iNOS proteins.

ATP Mediates Down-Regulation of AT_1R Signaling in Pressure-Overloaded Mouse Hearts. We finally examined whether ATP-induced AT_1R down-regulation occurred in vivo. We have previously reported that nucleotides (such as ATP and UDP) released from cardiac myocytes stimulate the production of fibrotic genes, which activate the production of collagen in cardiac fibroblasts in pressure overload-induced mice (24). As nucleotides are released from cardiac myocytes and the expression levels of AT_1Rs in cardiac fibroblasts are higher than those in cardiac myocytes, both cardiac myocytes and fibroblasts were cocultured on a silicone rubber dish. Mechanical stretch that stimulates nucleotides release from cardiac myocytes (24) decreased AT_1R density, which was canceled by pretreatment with L-NAME (Fig. 5*A*). As expected, inhibition of $P2Y_2R$ by PPADS or $P2Y_2R$ siRNA completely abolished mechanical stretch-induced AT_1R down-regulation. Mechanical stretch of cardiac cells induced ATP release, which leads to NO production in $P2Y_2R$ and iNOS-dependent manners (Fig. 5 *B* and *C*). Furthermore, 6 wk of transverse aortic constriction (TAC) induced significant increases in iNOS mRNA and protein levels and S-nitrosylation of p65, which were completely suppressed by the treatment with suramin, a P2 receptor antagonist (Fig. 5 *D* and *E*). Pressure overload also increased expression levels of eNOS proteins, but this increase was not affected by suramin. In addition, 6 wk of TAC decreased expression levels of AT_1R mRNA and proteins, which were also abolished by suramin treatment (Fig. 5 *E* and *F*). Furthermore, pressure overload-induced S-nitrosylation of p65 was diminished in iNOS knockout mouse hearts (Fig. 5 *G* and *H*) and in 1400W-treated mouse hearts (Fig. S10). These results suggest that mechanical stretch-induced ATP release causes AT_1R down-regulation through iNOS-dependent S-nitrosylation of p65 in pressure overloaded mice.

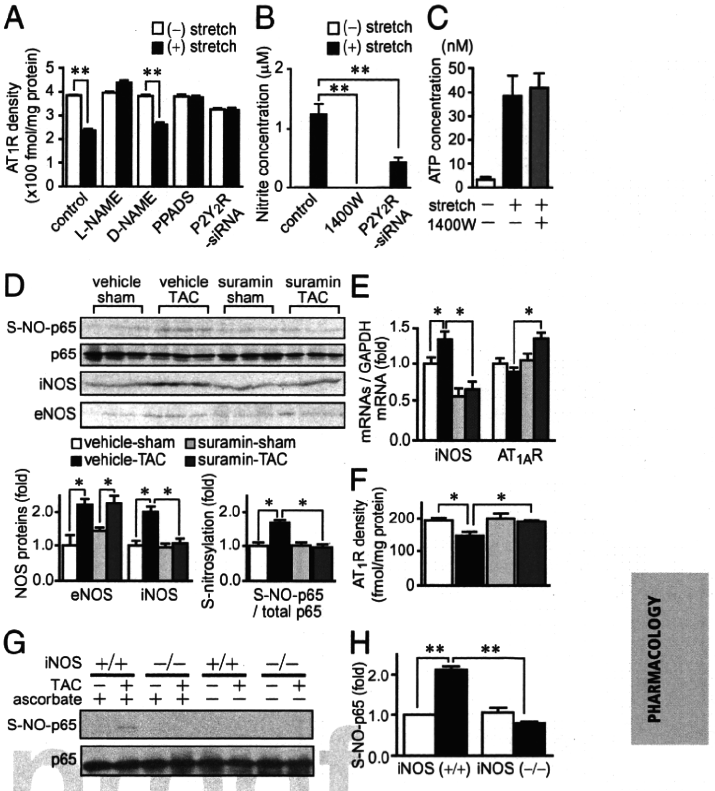

Fig. 5. Mechanical stretch induces AT_1R down-regulation through ATP-induced S-nitrosylation of NF-κB. (*A*) Effects of L-NAME (100 μM), D-NAME (100 μM), PPADS (100 μM), and $P2Y_2R$ siRNA on mechanical stretch-induced decrease in AT_1R density in rat cardiac myocytes. (*B*) Effects of 1400W (10 μM) and $P2Y_2R$ siRNA on mechanical stretch-induced nitrite production. (*C*) Effects of 1400W on mechanical stretch-induced ATP release (n = 3–5). (*D–F*) S-nitrosylation of p65, changes in expression of iNOS, p65, eNOS and AT_1R proteins induced by pressure overload in the presence or absence of suramin in mouse hearts. (*E*) Changes in iNOS and $AT_{1A}R$ mRNAs induced by TAC. (*F*) Changes in AT_1R density induced by TAC in the presence or absence of suramin (n = 3–6). (*G* and *H*) S-nitrosylation of p65 induced by pressure overload in wild type ($^{+/+}$) and iNOS-knockout ($^{-/-}$) mouse hearts. Tissue lysates were treated with or without ascorbate (1 mM) for 1 h (n = 3). $^*P < 0.05$, $^{**}P < 0.01$.

Discussion

A large number of studies have shown that a wide range of physiological and pathological stimuli modulate AT_1R expression in a number of cell types and tissues (40). We first demonstrated that ATP induces down-regulation of AT_1R signaling in rat cardiac fibroblasts. Extracellular ATP in the cardiovascular system may be originated from various cellular sources: perivascular sympathetic nerve endings, myocytes, endothelial cells, and inflammatory cells (14). We found that mechanical stretch-induced ATP release decreases AT_1R density in mouse hearts with pressure overload (Fig. 5). Although both ATP and Ang II are believed to function as an inflammatory factor (41), our results suggest that $P2Y_2R$-stimulated iNOS expression negatively regulates Ang II-mediated inflammatory response of the heart. We have previously reported that nucleotides released from cardiac myocytes activate $P2Y_6R$ of cardiac myocytes and induce fibrotic genes (24). In addition, Braun et al. has recently reported that $P2Y_2R$ stimulation by UTP induces fibrotic responses of cardiac fibroblasts (42). Thus, extracellular nucleotides contribute to cardiac fibrosis at least two independent pathways: one is induction of fibrotic genes in cardiac myocytes through $P2Y_6R$ and another is iNOS-mediated signaling in cardiac fibroblasts through $P2Y_2R$. The pathophysiological roles of $P2Y_2R$ signaling in the heart are still unclear, but our findings will provide a unique insight into the cross-talk between purinergic signaling and Ang II signaling in cardiovascular systems.

We revealed that local production of NO induces S-nitrosylation of NF-κB p65 and suppresses AT_1R transcription leading to down-regulation of AT_1R. Several reports have suggested the involvement of S-nitrosylation in NO-dependent (but cGMP independent) regulation of β-adrenergic receptor desensitization (12, 13). Most studies have shown the involvement of S-nitrosylation by exposing excessive concentration of NO to the cell, but we clearly show that NO produced by G_qPCR stimulation induces S-nitrosylation of NF-κB p65. In addition, this S-nitrosylation requires the functional interaction between iNOS and p65 in the cytosol. Although IL-1β potently induces expression of iNOS, IL-1β did not suppress NF-κB activity. This may be explained by the evidence that p65 was not colocalized with iNOS by IL-1β stimulation (Fig. 4). Thus, the complex formation between NO donor and acceptor is a critical factor of spatiotemporal regulation of NO signaling induced by ATP stimulation.

In conclusion, we reveal that S-nitrosylation of p65 is required for heterologous down-regulation of G_q-coupled AT_1R by another G_q-coupled $P2Y_2R$ stimulation. Although it is generally thought that heterologous regulation of GPCRs is mediated by second

messenger-activated kinases, heterologous down-regulation of AT_1R by ATP did not require the kinase activation in which cysteine modification of transcriptional factor plays essential roles. Our findings will provide a unique insight into cross-talk between GPCR signaling pathways.

Materials and Methods

Q:14 Materials, recombinant adenoviruses, and culture of cardiac fibroblasts, animals and TAC surgery, measurement of NF-κB-luciferase and AT_1R-luciferase activity, measurement of extracellular ATP concentration and NO production, measurement of AT_1R and iNOS expressions, quantification of intracellular Ca^{2+} concentration, S-nitrosylation biotin switch assay, immunoprecipitation, confocal visualization of NF-κB p65 subunit and iNOS proteins and statistical analysis are described in *SI Materials and Methods*.

ACKNOWLEDGMENTS. We thank K. Watanabe and A. Uemura for TAC operation. This study was supported by grants from Grant-in-Aid for Scientific Research on Innovative Areas (to M. Nishida); from the Ministry of Education, Culture, Sports, Science, and Technology of Japan (M. Nishida, M. Nakaya, and H.K.); and from Naito Foundation and Mochida Memorial Foundation (M. Nishida).

1. Pierce KL, Premont RT, Lefkowitz RJ (2002) Seven-transmembrane receptors. *Nat Rev Mol Cell Biol* 3:639–650.
2. Rockman HA, Koch WJ, Lefkowitz RJ (2002) Seven-transmembrane-spanning receptors and heart function. *Nature* 415:206–212.
3. Philipp M, Hein L (2004) Adrenergic receptor knockout mice: Distinct functions of 9 receptor subtypes. *Pharmacol Ther* 101:65–74.
4. Lefkowitz RJ (1998) G protein-coupled receptors. III. New roles for receptor kinases and β-arrestins in receptor signaling and desensitization. *J Biol Chem* 273: 18677–18680.
5. Pitcher JA, Freedman NJ, Lefkowitz RJ (1998) G protein-coupled receptor kinases. *Annu Rev Biochem* 67:653–692.
6. Chuang TT, Iacovelli L, Sallese M, De Blasi A (1996) G protein-coupled receptors: Heterologous regulation of homologous desensitization and its implications. *Trends Pharmacol Sci* 17:416–421.
7. de Gasparo M, Catt KJ, Inagami T, Wright JW, Unger T (2000) International union of pharmacology. XXIII. The angiotensin II receptors. *Pharmacol Rev* 52:415–472.
8. Wassman S, Nickenig G (2006) Pathophysiological regulation of the AT1-receptor and implications for vascular disease. *J Hypertens* 24:515–521.
9. Nickenig G, et al. (2002) Destabilization of AT(1) receptor mRNA by calreticulin. *Circ Res* 90:53–58.
10. Lima B, Forrester MT, Hess DT, Stamler JS (2010) S-nitrosylation in cardiovascular signaling. *Circ Res* 106:633–646.
11. Jaffrey SR, Erdjument-Bromage H, Ferris CD, Tempst P, Snyder SH (2001) Protein S-nitrosylation: A physiological signal for neuronal nitric oxide. *Nat Cell Biol* 3:193–197.
12. Whalen EJ, et al. (2007) Regulation of β-adrenergic receptor signaling by S-nitrosylation of G-protein-coupled receptor kinase 2. *Cell* 129:511–522.
13. Ozawa K, et al. (2008) S-nitrosylation of β-arrestin regulates β-adrenergic receptor trafficking. *Mol Cell* 31:395–405.
14. Lander HM, et al. (1996) Redox regulation of cell signalling. *Nature* 381:380–381.
15. Nishida M, et al. (2002) Activation mechanism of G_i and G_o by reactive oxygen species. *J Biol Chem* 277:9036–9042.
16. Ichiki T, et al. (1998) Downregulation of angiotensin II type 1 receptor gene transcription by nitric oxide. *Hypertension* 31:342–348.
17. Porter KE, Turner NA (2009) Cardiac fibroblasts: At the heart of myocardial remodeling. *Pharmacol Ther* 123:255–278.
18. Onohara N, et al. (2006) TRPC3 and TRPC6 are essential for angiotensin II-induced cardiac hypertrophy. *EMBO J* 25:5305–5316.
19. Fujii T, et al. (2005) Galpha12/13-mediated production of reactive oxygen species is critical for angiotensin receptor-induced NFAT activation in cardiac fibroblasts. *J Biol Chem* 280:23041–23047.
20. Molkentin JD, et al. (1998) A calcineurin-dependent transcriptional pathway for cardiac hypertrophy. *Cell* 93:215–228.
21. Erlinge D, Burnstock G (2008) P2 receptors in cardiovascular regulation and disease. *Purinergic Signal* 4:1–20.
22. Koizumi S, et al. (2007) UDP acting at $P2Y_6$ receptors is a mediator of microglial phagocytosis. *Nature* 446:1091–1095.
23. Seye CI, et al. (2002) Functional $P2Y_2$ nucleotide receptors mediate uridine 5′-triphosphate-induced intimal hyperplasia in collared rabbit carotid arteries. *Circulation* 106:2720–2726.
24. Nishida M, et al. (2008) P2Y6 receptor-Galpha12/13 signalling in cardiomyocytes triggers pressure overload-induced cardiac fibrosis. *EMBO J* 27:3104–3115.
25. Lai MM, Burnett PE, Wolosker H, Blackshaw S, Snyder SH (1998) Cain, a novel physiologic protein inhibitor of calcineurin. *J Biol Chem* 273:18325–18331.
26. Wu H, Peisley A, Graef IA, Crabtree GR (2007) NFAT signaling and the invention of vertebrates. *Trends Cell Biol* 17:251–260.
27. Tang CM, Insel PA (2004) GPCR expression in the heart; "new" receptors in myocytes and fibroblasts. *Trends Cardiovasc Med* 14:94–99.
28. Cowling RT, Gurantz D, Peng J, Dillmann WH, Greenberg BH (2002) Transcription factor NF-κ B is necessary for up-regulation of type 1 angiotensin II receptor mRNA in rat cardiac fibroblasts treated with tumor necrosis factor-α or interleukin-1 β. *J Biol Chem* 277:5719–5724.
29. Nishida M, et al. (2010) *Pertussis* toxin up-regulates angiotensin type 1 receptors through Toll-like receptor 4-mediated Rac activation. *J Biol Chem* 285:15268–15277.
30. Taylor BS, et al. (1998) Multiple NF-kappaB enhancer elements regulate cytokine induction of the human inducible nitric oxide synthase gene. *J Biol Chem* 273: 15148–15156.
31. Obasanjo-Blackshire K, et al. (2006) Calcineurin regulates NFAT-dependent iNOS expression and protection of cardiomyocytes: Co-operation with Src tyrosine kinase. *Cardiovasc Res* 71:672–683.
32. Ghosh S, Hayden MS (2008) New regulators of NF-kappaB in inflammation. *Nat Rev Immunol* 8:837–848.
33. Kelleher ZT, Matsumoto A, Stamler JS, Marshall HE (2007) NOS2 regulation of NF-kappaB by S-nitrosylation of p65. *J Biol Chem* 282:30667–30672.
34. Marshall HE, Stamler JS (2001) Inhibition of NF-κ B by S-nitrosylation. *Biochemistry* 40: 1688–1693.
35. Buss H, et al. (2004) Phosphorylation of serine 468 by GSK-3β negatively regulates basal p65 NF-kappaB activity. *J Biol Chem* 279:49571–49574.
36. Knowles RG, Moncada S (1994) Nitric oxide synthases in mammals. *Biochem J* 298: 249–258.
37. Gao H, et al. (2004) Identification of β-arrestin2 as a G protein-coupled receptor-stimulated regulator of NF-kappaB pathways. *Mol Cell* 14:303–317.
38. Witherow DS, Garrison TR, Miller WE, Lefkowitz RJ (2004) β-Arrestin inhibits NF-kappaB activity by means of its interaction with the NF-kappaB inhibitor IkappaBalpha. *Proc Natl Acad Sci USA* 101:8603–8607.
39. Kuhr FK, Zhang Y, Brovkovych V, Skidgel RA (2010) β-arrestin 2 is required for B1 receptor-dependent post-translational activation of inducible nitric oxide synthase. *FASEB J* 24:2475–2483.
40. Elton TS, Martin MM (2007) Angiotensin II type 1 receptor gene regulation: Transcriptional and posttranscriptional mechanisms. *Hypertension* 49:953–961.
41. Idzko M, et al. (2007) Extracellular ATP triggers and maintains asthmatic airway inflammation by activating dendritic cells. *Nat Med* 13:913–919.
42. Braun OO, Lu D, Aroonsakool N, Insel PA (2010) Uridine triphosphate (UTP) induces profibrotic responses in cardiac fibroblasts by activation of P2Y2 receptors. *J Mol Cell Cardiol* 49:362–369.

AUTHOR QUERIES

AUTHOR PLEASE ANSWER ALL QUERIES 1

Q: 1_Please contact PNAS_Specialist.djs@sheridan.com if you have questions about the editorial changes, this list of queries, or the figures in your article. Please include your manuscript number in the subject line of all e-mail correspondence; your manuscript number is 201017640. Please (i) review the author affiliation and footnote symbols carefully, (ii) check the order of the author names, and (iii) check the spelling of all author names and affiliations. Please indicate that the author and affiliation lines are correct by adding the comment "OK" next to the author line. Please note that this is your opportunity to correct errors in your article prior to publication. Corrections requested after online publication will be considered and processed as errata.

Q: 2_If your article contains links to Web sites (other than the SI links for your article), please verify that the links are valid and will direct readers to the proper Web page.

Q: 3_Author names may have been edited to match those provided during article submission; please check carefully and note your approval in the margin. (Your article cannot be published until your approval has been received.)

Q: 4_PNAS does not allow statements of novelty or priority. Unique has replaced novel. Please approve/ rewrite the edit here and below.

Q: 5_PNAS allows up to five key terms that (i) do not repeat terms present in the title or abstract (which are searchable online) and (ii) do not include nonstandard abbreviations. Please provide up to 5 new key terms that do not repeat terms present in the title or abstract and do not include nonstandard abbreviations. Because we prefer to avoid publishing a single key term, please add at least two terms (and specify your preferred order in which the terms should appear) if you add any terms.

Q: 6_Please review the information in the author contribution footnote carefully. Please make sure that the information is correct and that the correct author initials are listed. Note that the order of author initials matches the order of the author line per journal style. You may add contributions to the list in the footnote; however, funding should not be an author's only contribution to the work.

Q: 7_You will receive a notification from the PNAS eBill system in 1-2 days. Each corresponding author is required to log in to the system and provide payment information for applicable publication charges (purchase order number or credit card information) upon receipt of the notification. You will have the opportunity to order reprints through the eBill system if desired, as well. Failure to log in and provide the required information may result in publication delays.

Q: 8_Reminder: You have chosen not to pay an additional $1275 (or $950 if your institution has a site license) for the PNAS Open Access option.

Q: 9_interventional trials (rather than trails) as meant?

Q: 10_NFAT in cardiac fibroblasts is "fully unknown" as meant, which means completely unknown? Or is the intention "not fully (not completely) known?" Please change if needed.